THE UNIVERSITY OF TEXAS AT AUSTIN
MaterialsPhysicsLab
DEPARTMENT OF PHYSICS

Integration of Functional Oxides and Semiconductors:

Magnetism and Epitaxy

Alex Demkov
The University of Texas at Austin

Texas A&M University, Commerce, November 2013

People involved:

Hosung Seo

Miri Choi

Patrick Ponath

Kristy Kormondy

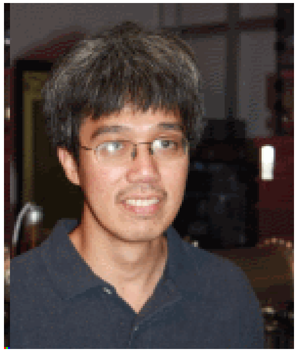

Agham Posadas

Chandrima Mitra

Chungwei Lin

Richard Hatch

Outline of the talk

- Introduction
- Magnetism in Oxides
- Molecular Beam Epitaxy
- COX
- $LaCoO_3$ on Si
- Conclusions

Advances in Oxide Epitaxy

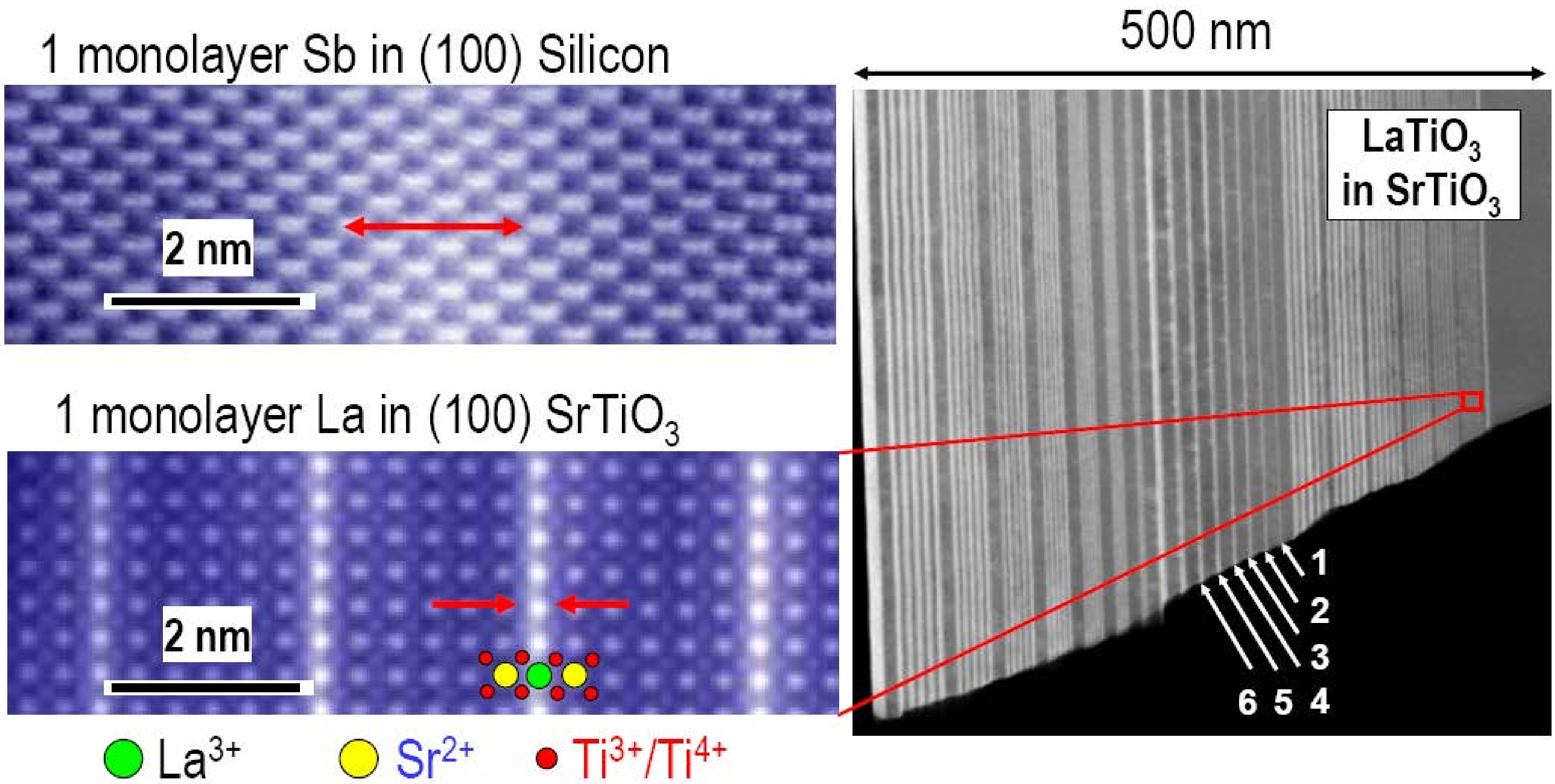

Superlattices by design

A. Ohtomo, D. A. Muller, J. A. Grazul, and H. Y. Hwang, *Nature* **419**, 378 (2002).

Epitaxial oxide on semiconductors

$BaTiO_3$ on Ge

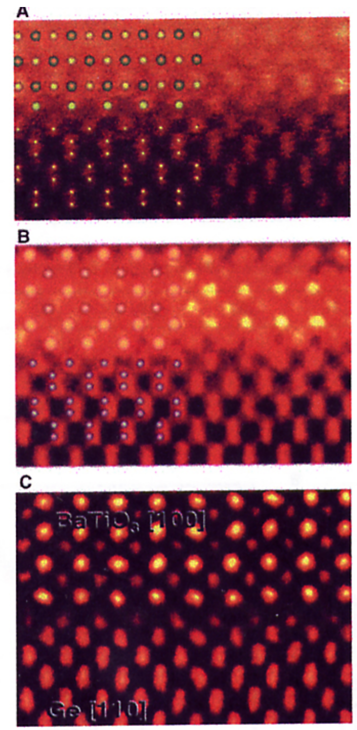

Fig. 1. Alkaline earth and perovskite oxide heteroepitaxy on silicon and germanium. The figure illustrates our ability to manipulate interface structure at the atomic level using our $(AO)_n(A'BO_3)_m$ structure series. The n/m ratio defines the electrical characteristics of this new physical system of COS in a MOS capacitor. In (**A**), $n = 3, m = 0$; in (**B**), $n = 1, m = 2$; in (**C**), $n = 0, m = 3$.

$SrTiO_3$ on Si

Model

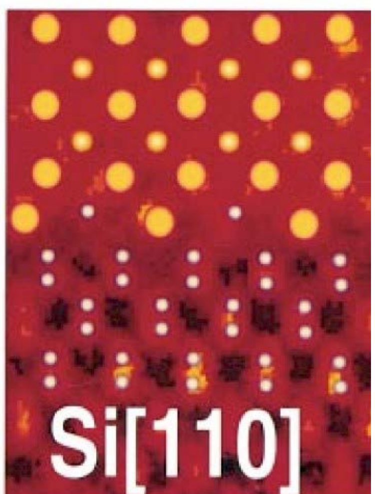

Experiment

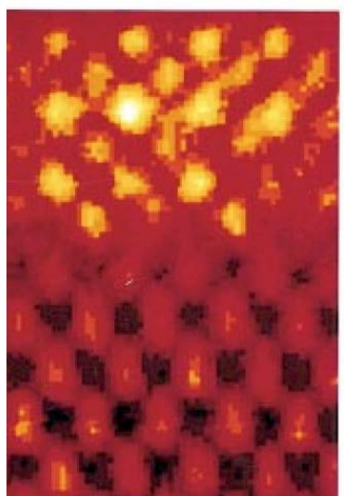

R. McKee, F. Walker, M. Chisholm, *PRL* 81 3014 (1998)
R. McKee, F. Walker, M. Chisholm, *Science 293, 468 (2001)*

$SrTiO_3/LaAlO_3$ heterostructure:

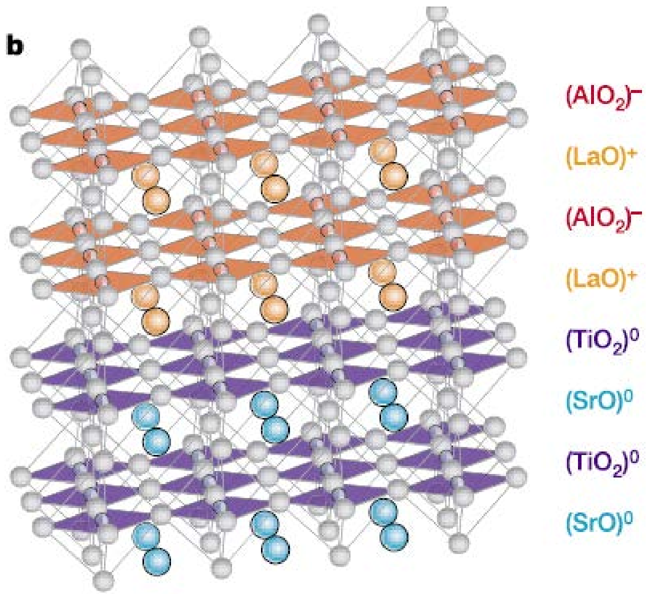

letters to nature

A high-mobility electron gas at the $LaAlO_3/SrTiO_3$ heterointerface

A. Ohtomo[1,2,3] & H. Y. Hwang[1,3,4]

[1] Bell Laboratories, Lucent Technologies, Murray Hill, New Jersey 07974, USA
[2] Institute for Materials Research, Tohoku University, Sendai, 980-8577, Japan
[3] Japan Science and Technology Agency, Kawaguchi, 332-0012, Japan
[4] Department of Advanced Materials Science, University of Tokyo, Kashiwa, Chiba, 277-8651, Japan

limit, this interface presents an extra half electron or hole per two-dimensional unit cell, depending on the structure of the interface. The hole-doped interface is found to be insulating, whereas the electron-doped interface is conducting, with extremely high carrier mobility exceeding 10,000 $cm^2 V^{-1} s^{-1}$. At low temperature, dramatic magnetoresistance oscillations periodic with the inverse magnetic field are observed, indicating quantum transport. These results present a broad opportunity to tailor low-dimensional charge states by atomically engineered oxide heteroepitaxy.

An early discussion of polarity or valence discontinuities arose in the consideration of the growth of GaAs on (001)-oriented Ge[1,2]. Both semiconductors have the same crystal structure and nearly

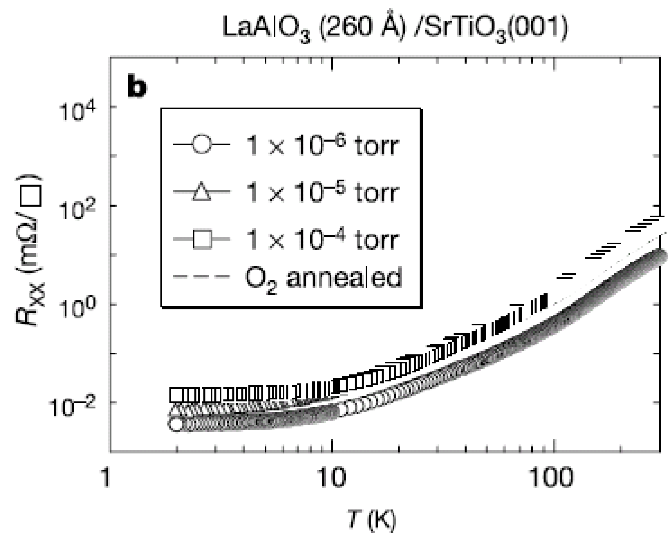

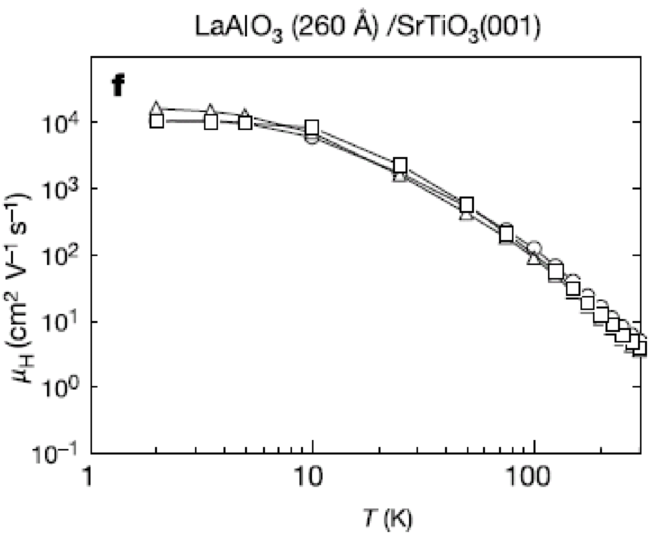

ARTICLES

Why some interfaces cannot be sharp

NAOYUKI NAKAGAWA[1,2], HAROLD Y. HWANG[1,2] AND DAVID A. MULLER[3]*

[1] Department of Advanced Materials Science, University of Tokyo, Kashiwa, Chiba 277-8561, Japan
[2] Japan Science and Technology Agency, Kawaguchi 332-0012, Japan
[3] School of Applied and Engineering Physics, Cornell University, Ithaca, New York 14583, USA
*e-mail: davidm@ccmr.cornell.edu

H. W. Hwang *et al.*, *Nature* 427, 423 (2004)
H. W. Hwang, Science 313, 1895 (2006)

Superconducting Interfaces Between Insulating Oxides

N. Reyren,[1] S. Thiel,[2] A. D. Caviglia,[1] L. Fitting Kourkoutis,[3] G. Hammerl,[2] C. Richter,[2] C. W. Schneider,[2] T. Kopp,[2] A.-S. Rüetschi,[1] D. Jaccard,[1] M. Gabay,[4] D. A. Muller,[3] J.-M. Triscone,[1] J. Mannhart[2]*

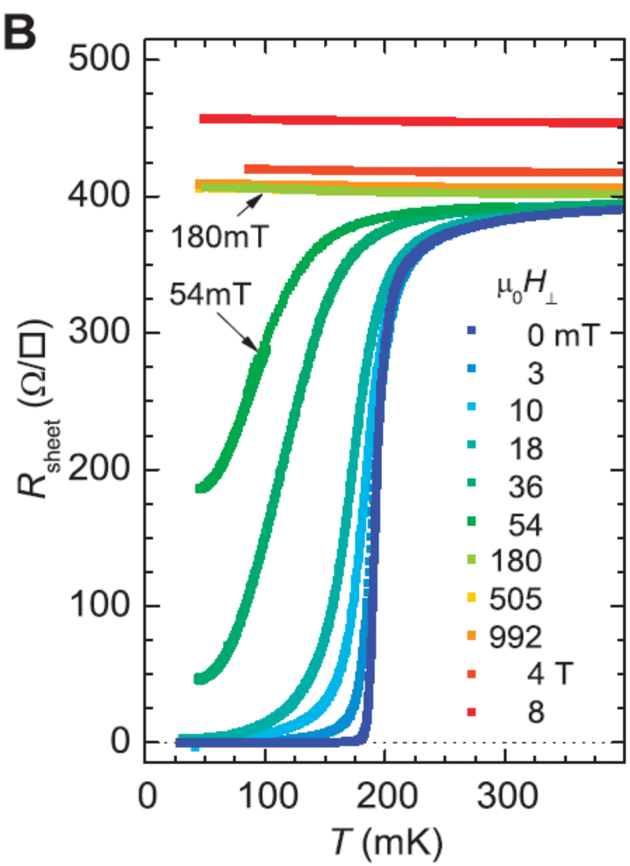

N. Reyren *et al*., *Science 317 1196* (2007)

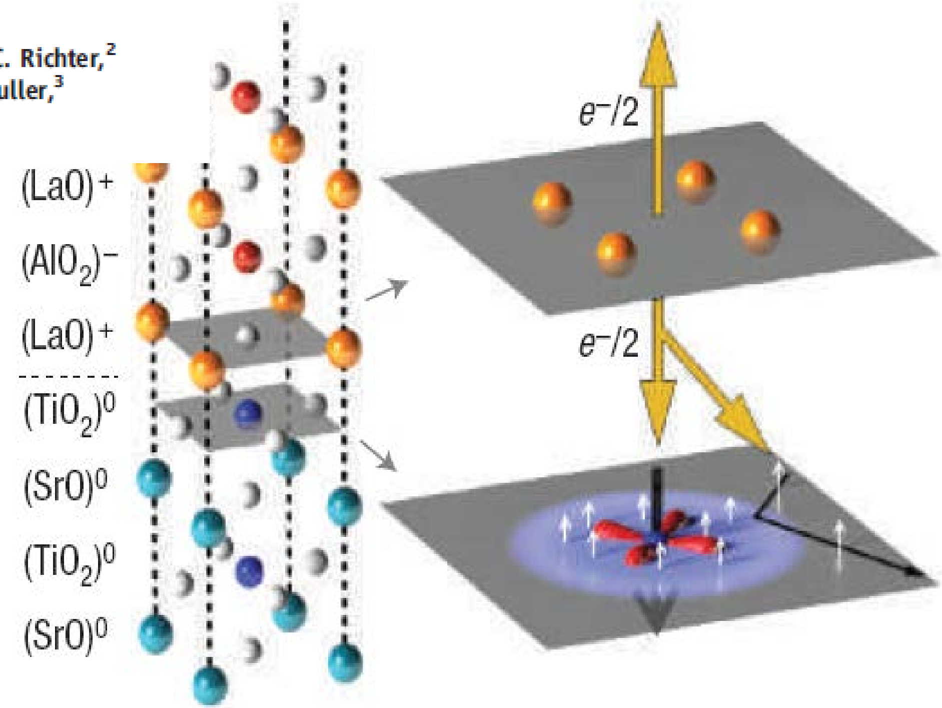

A. Brinkman *et al*., Nature Materials 6, 493 (2007)

LETTERS

Magnetic effects at the interface between non-magnetic oxides

A. BRINKMAN[1]*, M. HUIJBEN[1†], M. VAN ZALK[1], J. HUIJBEN[1], U. ZEITLER[2], J. C. MAAN[2], W. G. VAN DER WIEL[3], G. RIJNDERS[1], D. H. A. BLANK[1] AND H. HILGENKAMP[1]

[1]Faculty of Science and Technology and MESA+ Institute for Nanotechnology, University of Twente, 7500 AE Enschede, The Netherlands
[2]High Field Magnet Laboratory, Institute for Molecules and Materials, Radboud University Nijmegen, 6525 ED Nijmegen, The Netherlands
[3]Strategic Research Orientation NanoElectronics, MESA+ Institute for Nanotechnology, University of Twente, 7500 AE Enschede, The Netherlands
†Present address: Physics Department, University of California, Berkeley, California 94720, USA
*e-mail: a.brinkman@utwente.nl

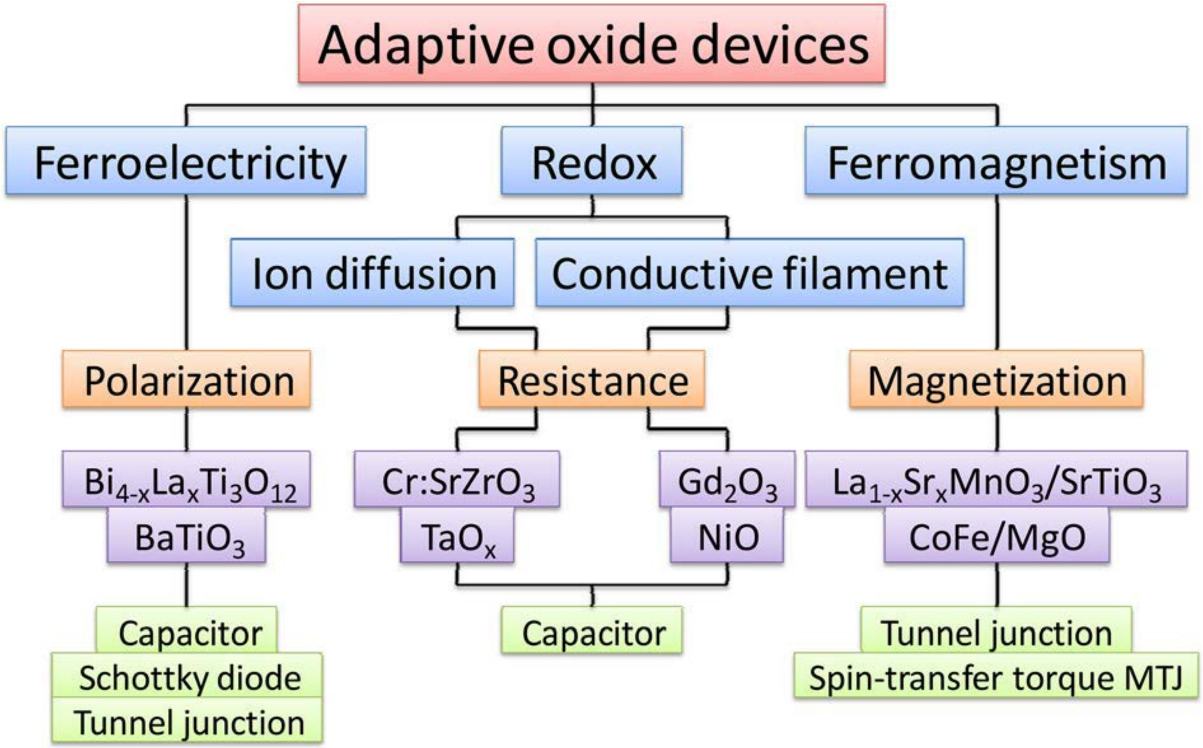
Adaptive oxide devices
Ferroelectricity
Redox
Ferromagnetism
Ion diffusion
Conductive filament
Polarization
Resistance
Magnetization
$Bi_{4-x}La_xTi_3O_{12}$
$BaTiO_3$
$Cr:SrZrO_3$
TaO_x
Gd_2O_3
NiO
$La_{1-x}Sr_xMnO_3/SrTiO_3$
CoFe/MgO
Capacitor
Schottky diode
Tunnel junction
Capacitor
Tunnel junction
Spin-transfer torque MTJ

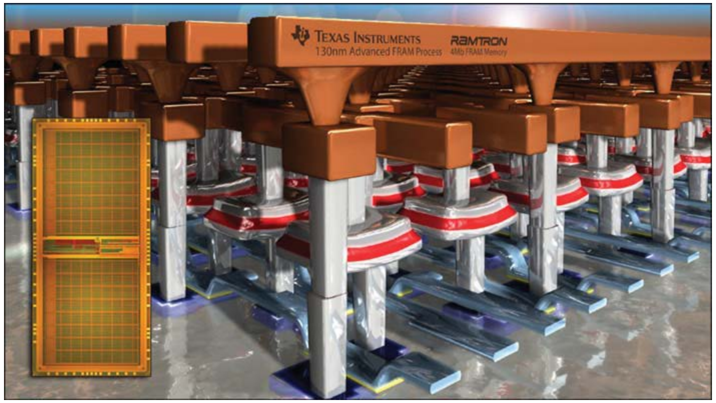
TEXAS INSTRUMENTS
130nm Advanced FRAM Process
RAMTRON

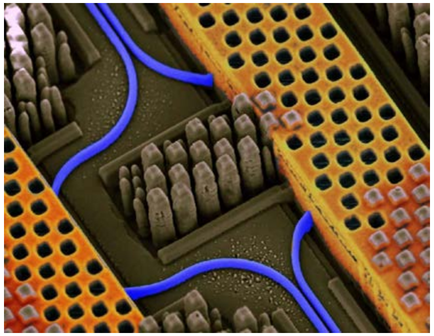

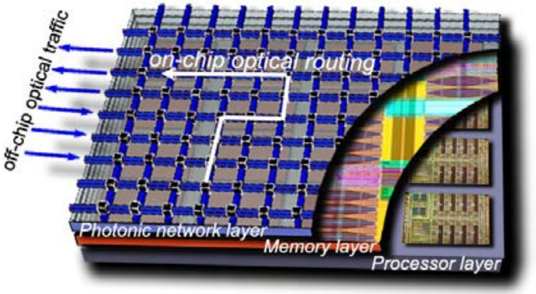
off-chip optical traffic
on-chip optical routing
Photonic network layer
Memory layer
Processor layer

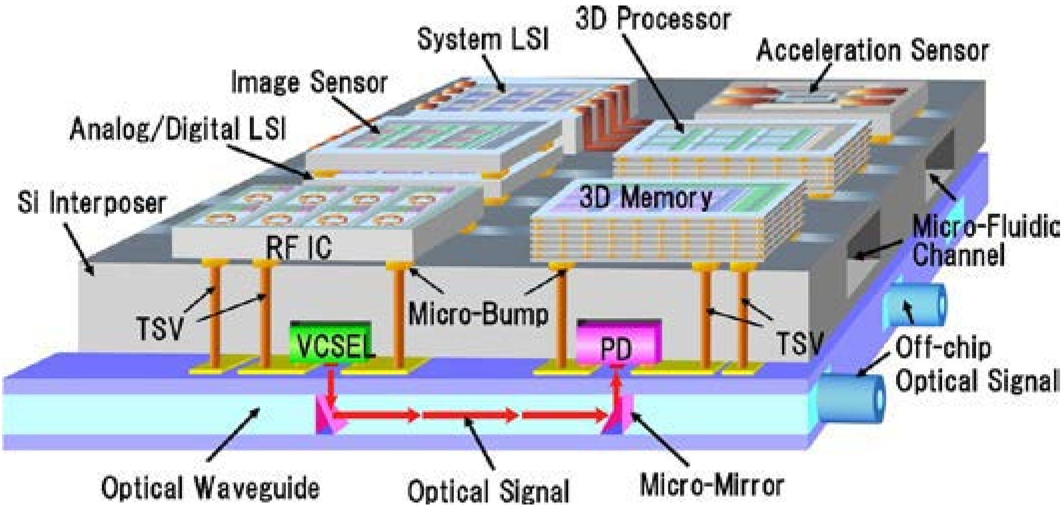

Conceptual structure of the 3-D heterogeneous optoelectronic integrated system-on-silicon for an intelligent vehicle system's variable signal-processing functions depending on the moving speed of the car.
K.-W. Lee, A. Noriki, K. Kiyoyama, T. Fukushima, T. Tanaka, and M. Koyanagi, *IEEE Trans. Electron Dev.* **58**, 748 (2011).

Diverse Accessible Heterogeneous Integration (DAHI):

- Compound Semiconductor Materials on Si,
- Electronic-photonic heterogeneous integration

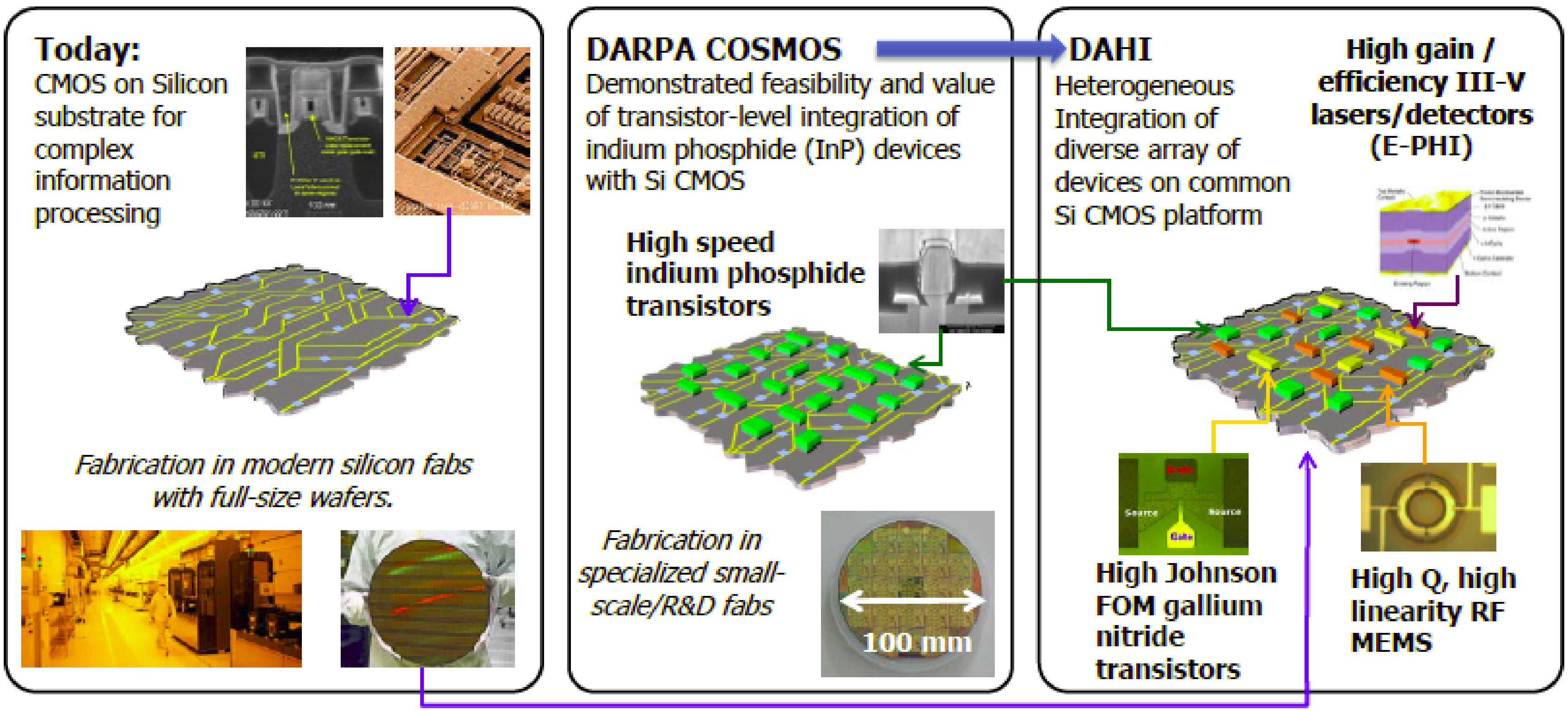

Transition metals

A transition metal is one which forms one or more stable ions which have ***incompletely filled d orbitals***.

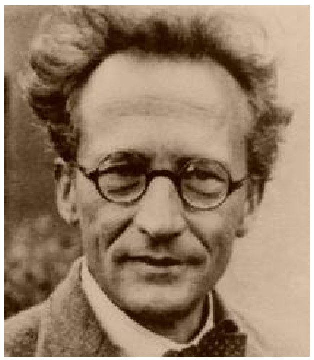

Erwin Schrödinger

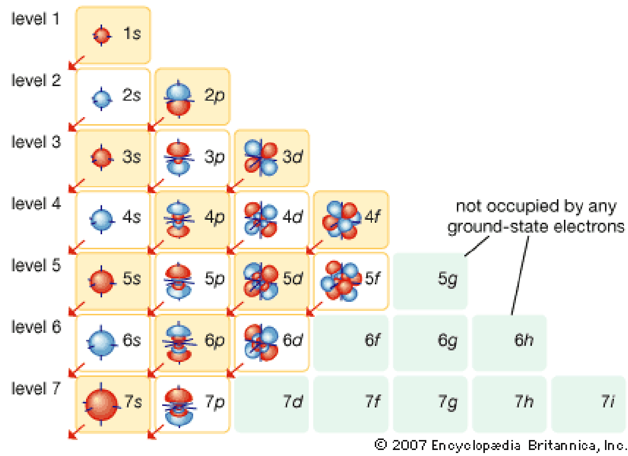

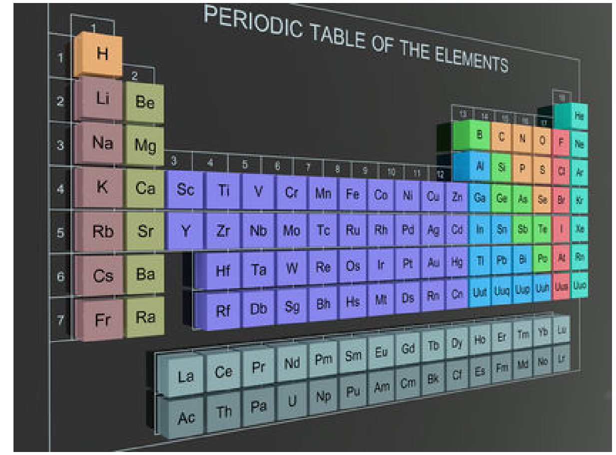

$[Ar] = 1s^2\ 2s^2\ 2p^6\ 3s^2\ 3p^6$

$[Ti] = [Ar]3d^2 4s^2$

$[V] = [Ar]3d^3 4s^2$

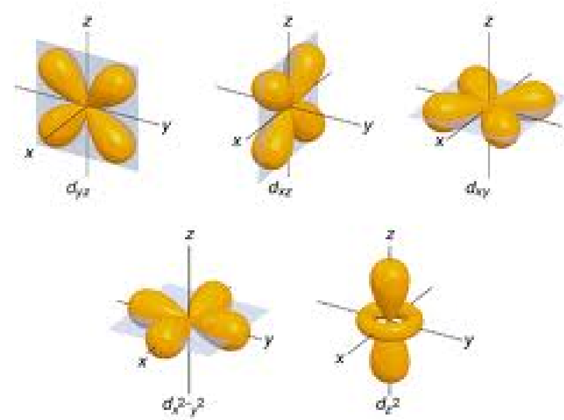

Perovskite oxides ABO_3

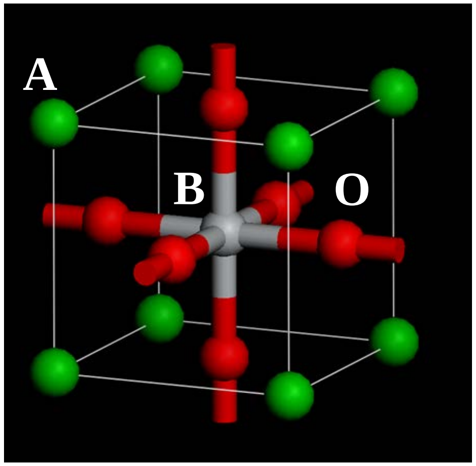

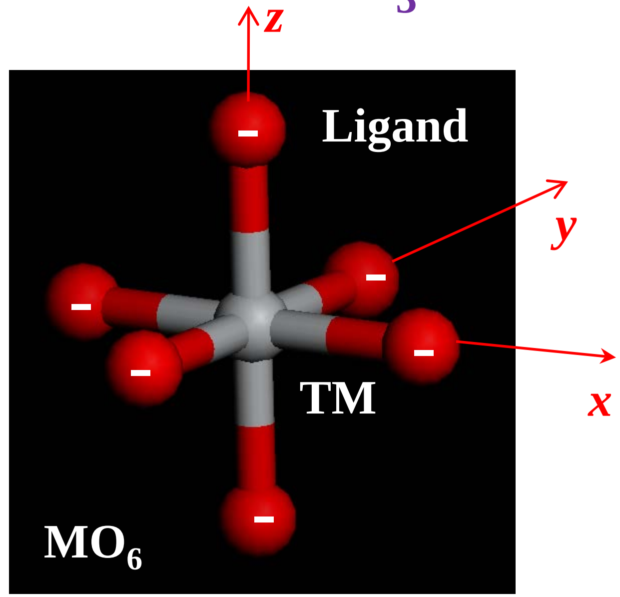

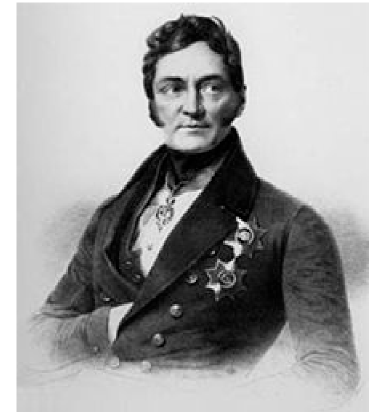

Count Lev Alekseevich Perovski
1792-1856

$CaTiO_3$, $BaTiO_3$, $SrHfO_3$,…

Octahedral symmetry (O_h):

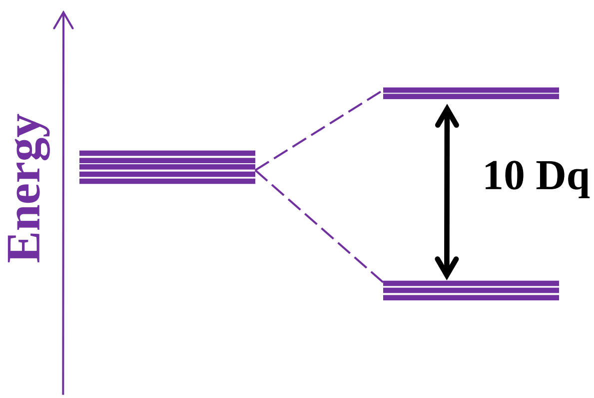

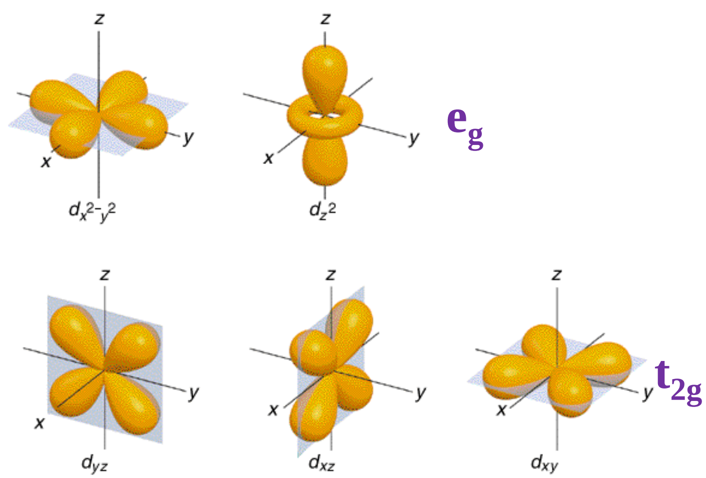

High spin Low spin

Fe^{3+} (d^5)

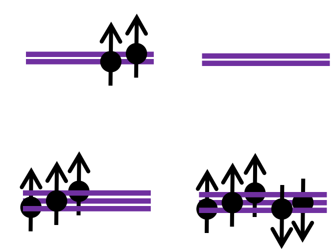

$E^S-E^T=2J$

Ligand field theory

Molecular Orbital Theory

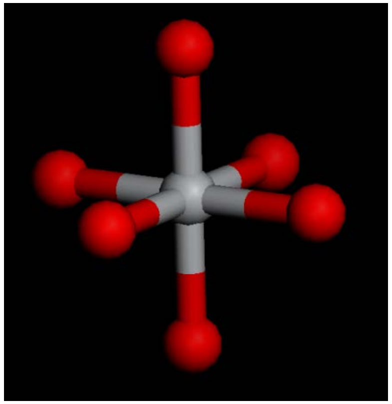

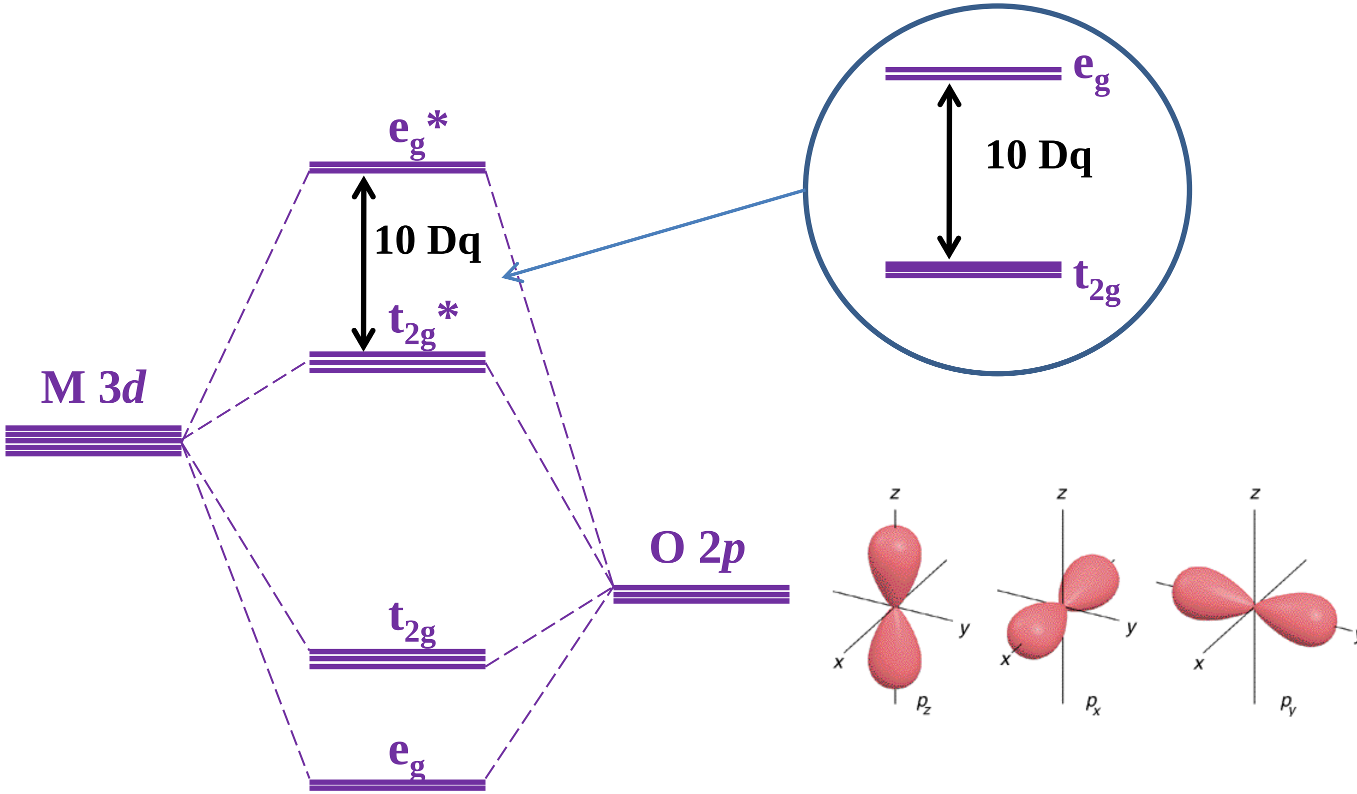

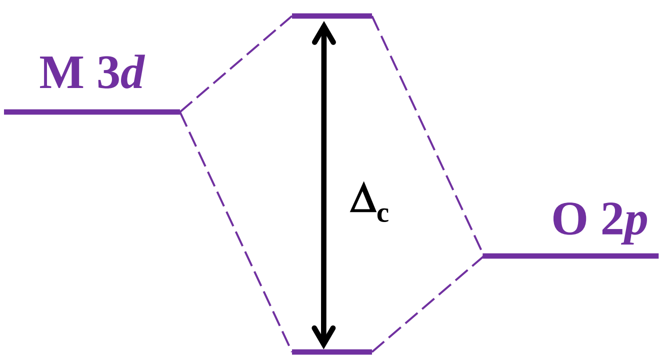

Important energies:

- crystal filed splitting 10Dq
- exchange energy J
- charge transfer energy Δ_c

Ferroelectricity

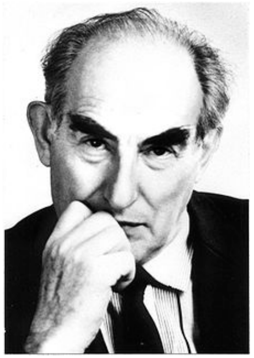

V.L. Ginzburg
1916-2009

L.D. Landau
1908-1968

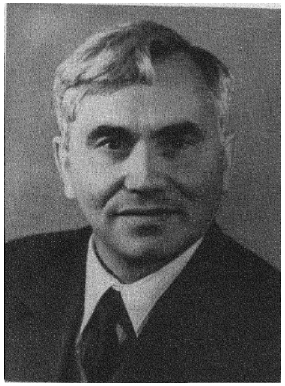

B.M. Vul
1903-1985

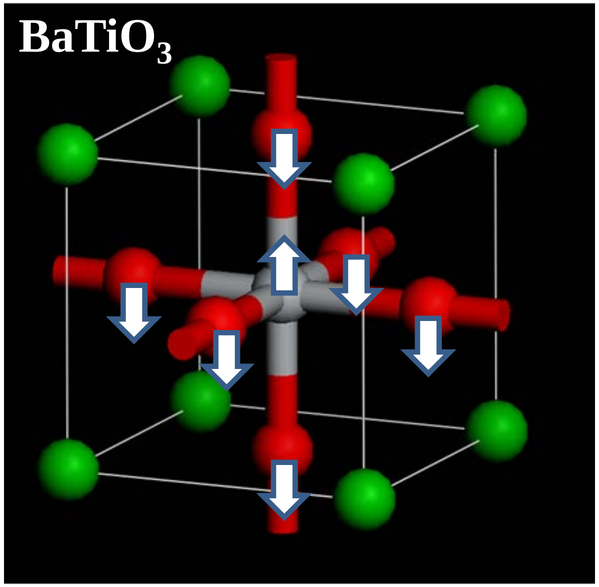

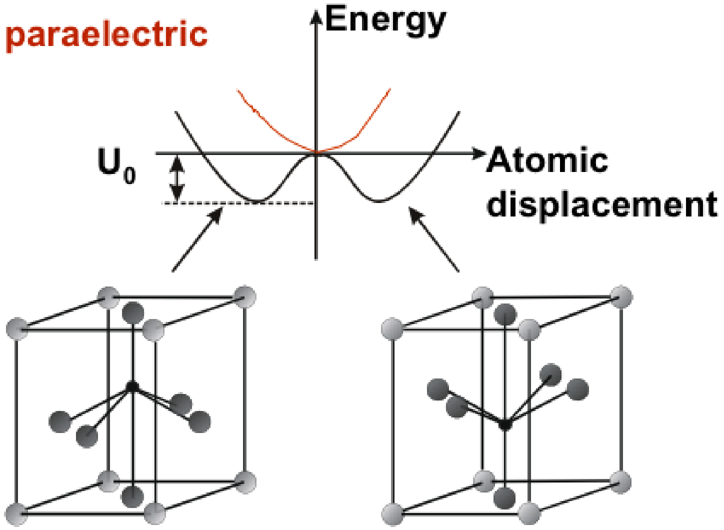

$$\Delta E = \frac{1}{2}\alpha_0 \left(T - T_0\right) P_x^2 + \frac{1}{4}\alpha_{11} P_x^4 + \frac{1}{6}\alpha_{111} P_x^6$$

Molecular Beam Epitaxy

Epitaxy: ordered growth on a monocrystalline substrate

From two Greek words: “epi”-above and “taxis”-in ordered manner

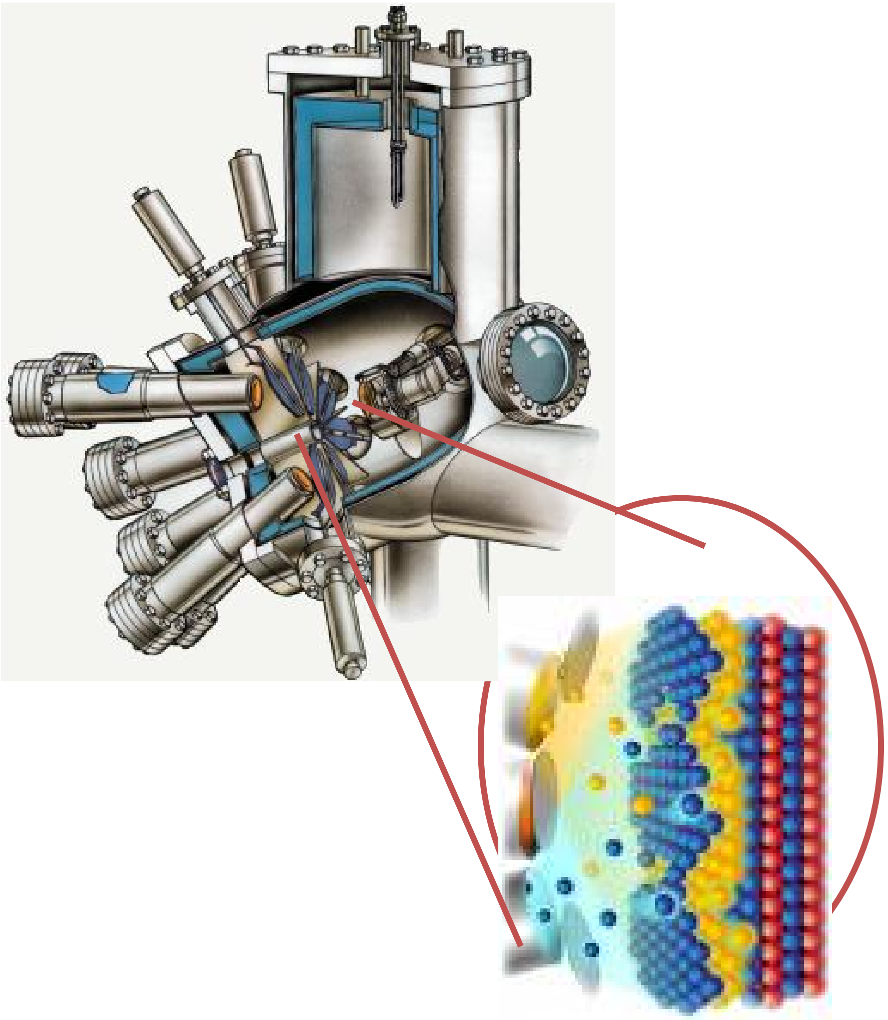

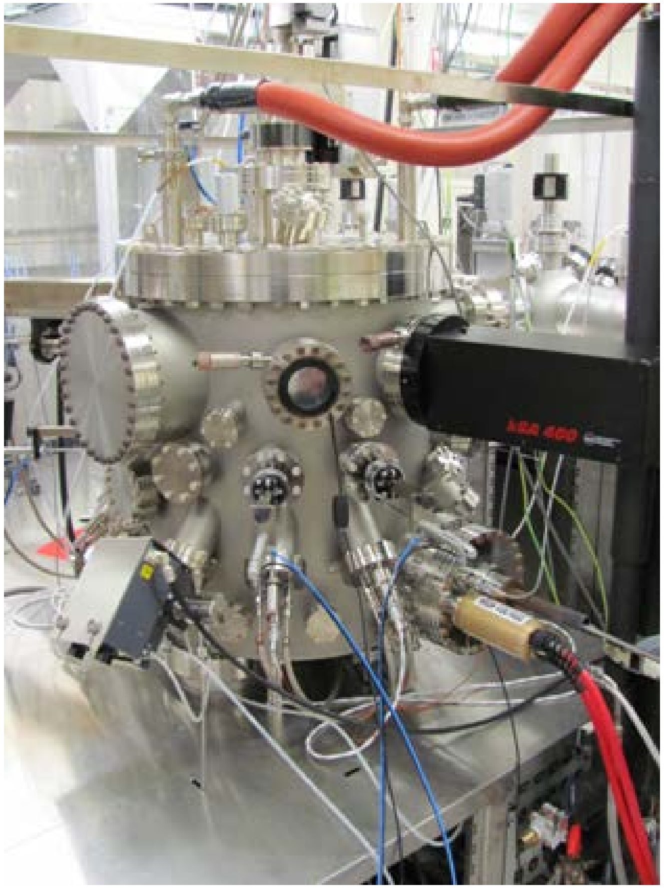

MBE was invented in the late 1960s at Bell Laboratories by J. R. Arthur and Alfred Y. Cho

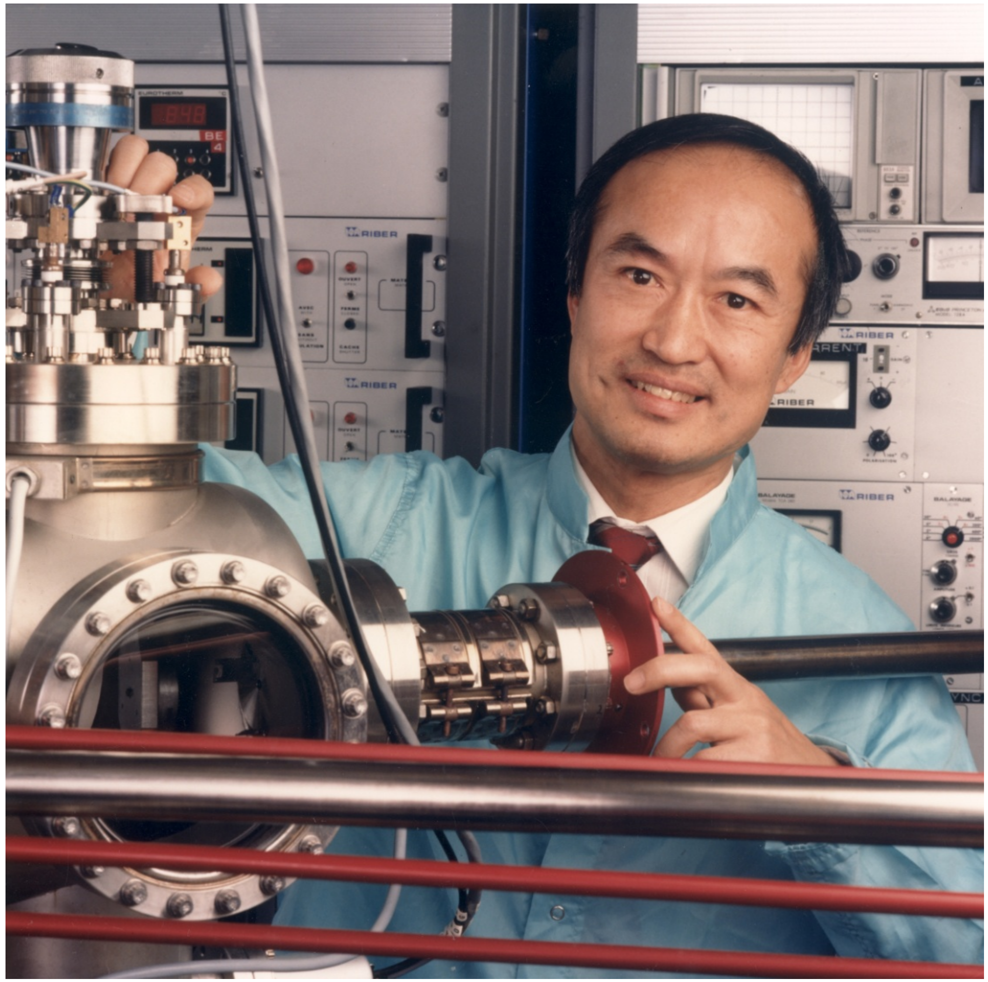

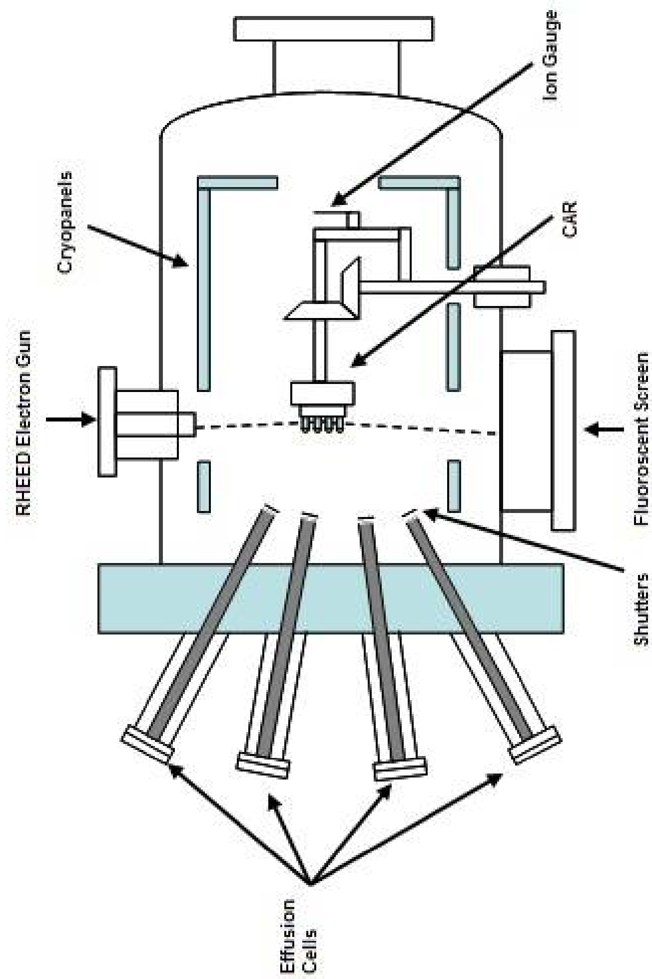
Ion Gauge
Cryopanels
CAR
RHEED Electron Gun
Fluoroscent Screen
Shutters
Effusion Cells

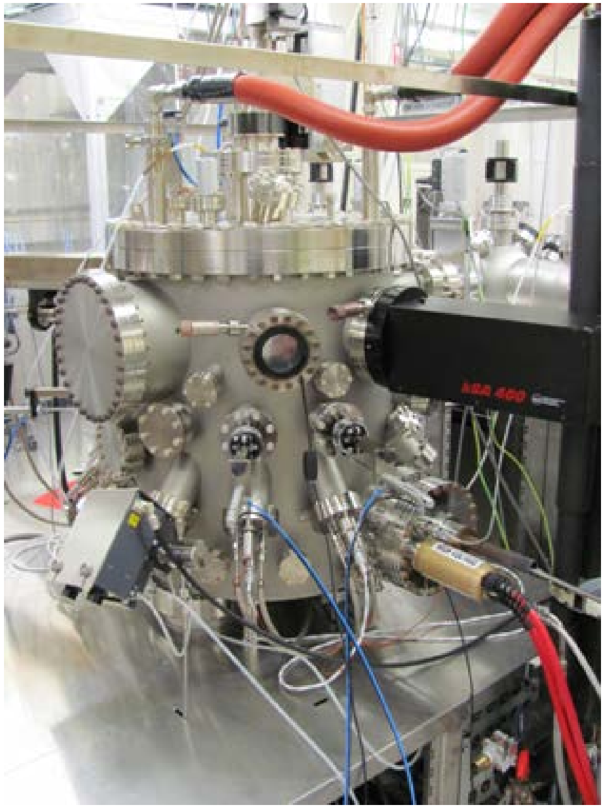

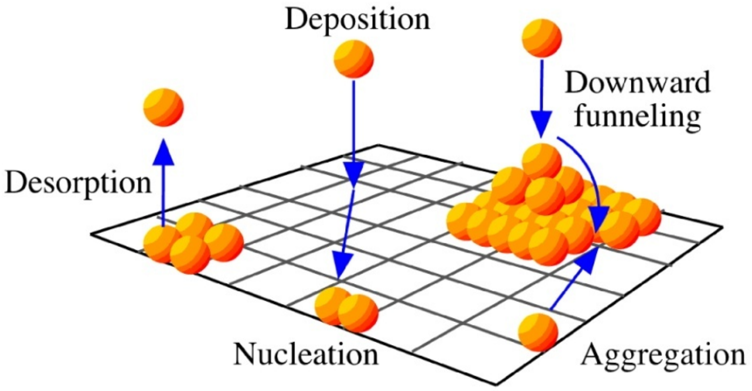
Deposition
Downward funneling
Desorption
Nucleation
Aggregation

Making Nothing: Vacuum Pumps

10^{-2} -10^{-3} Torr

10^{-2} -10^{-10} Torr

10^{-7} -10^{-11} Torr

10^{-3} -10^{-7} Torr

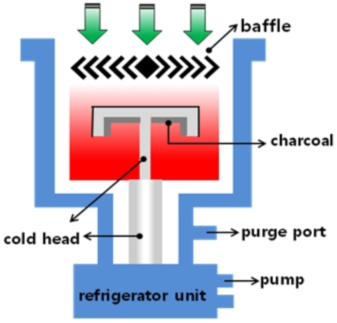

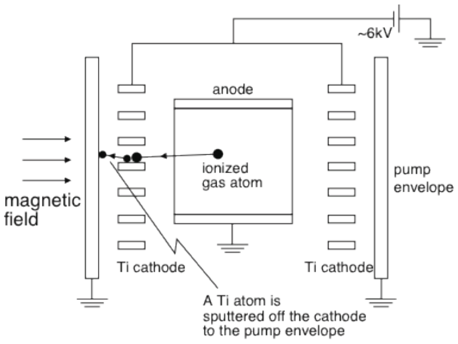

Vacuum Chamber

Flanges

Manipulators

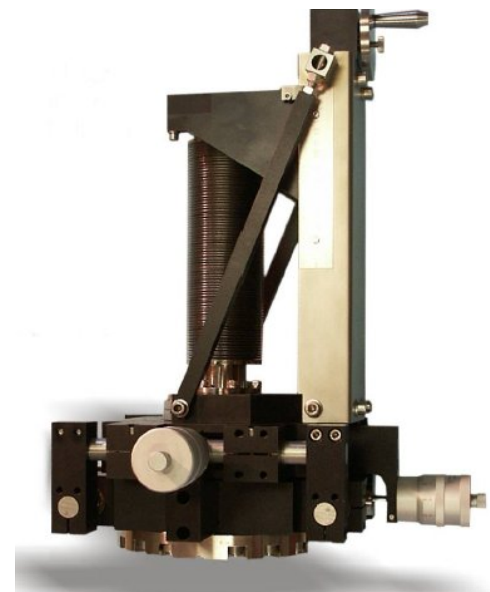

Vacuum gauges

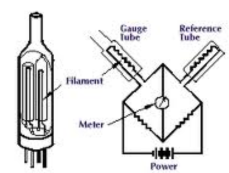

Transfer rods

Knudsen Cell

Martin Hans Christian Knudsen (1871 -1949)

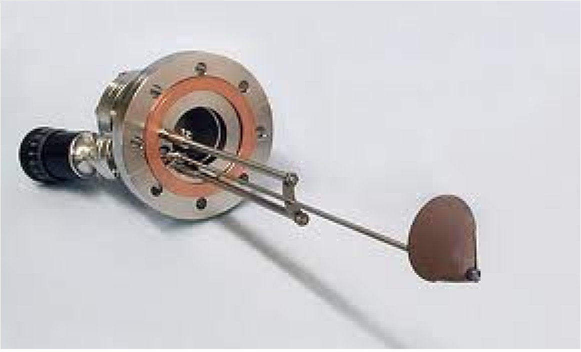

E-gun evaporator

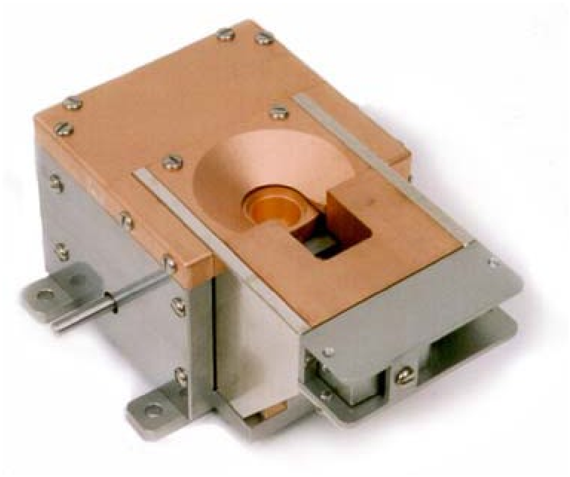

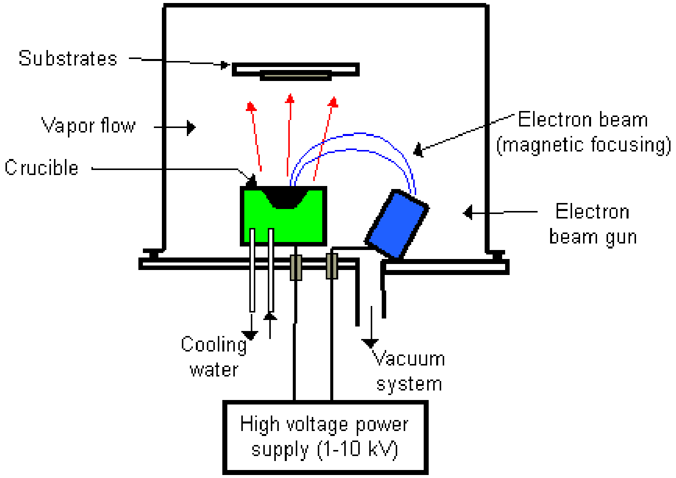

Quartz Crystal Monitor

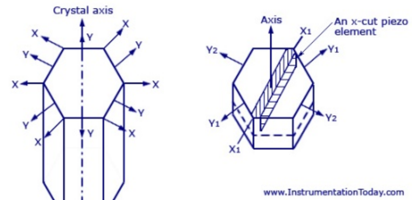

X-Y axes of a piezoelectric crystal

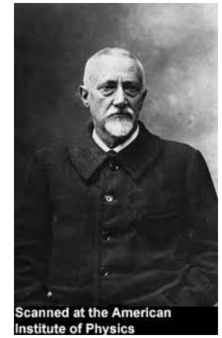

Jacques Curie


Pierre Curie

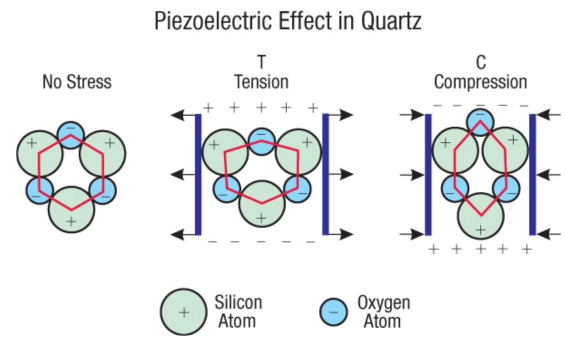

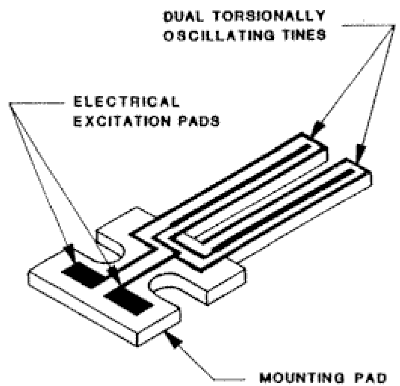

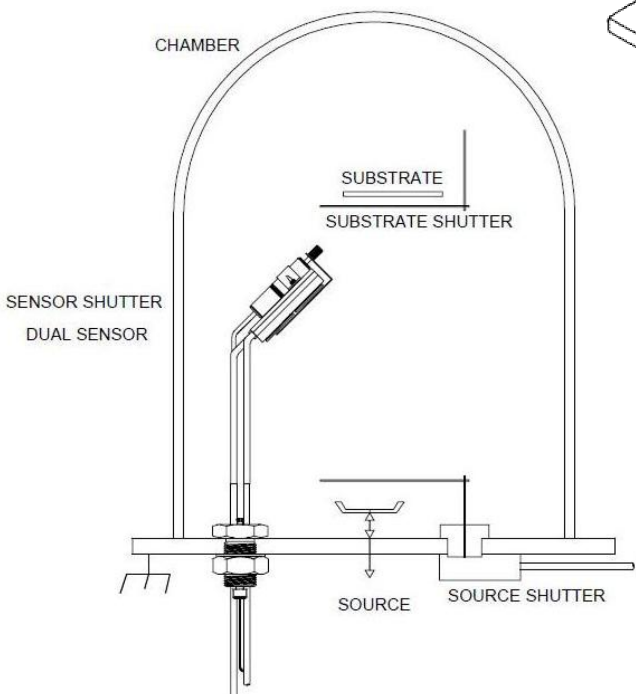

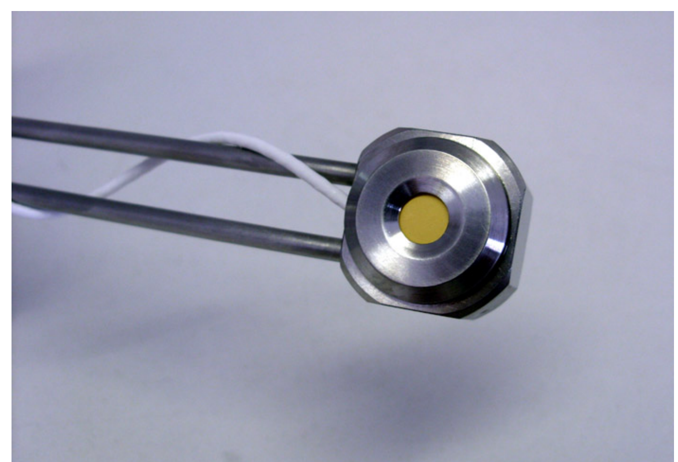

RHEED

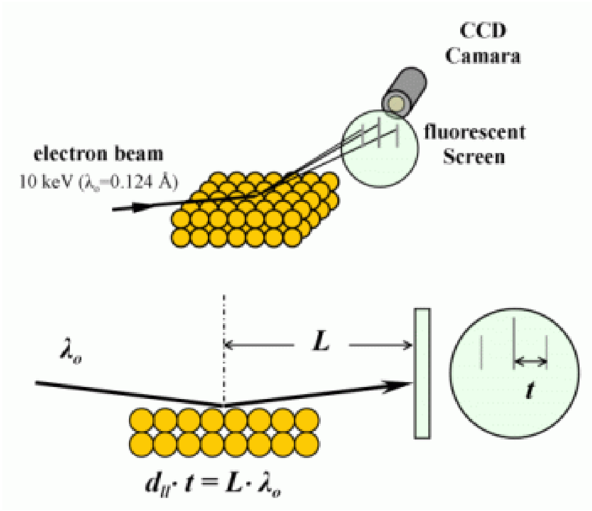

CCD
Camara
fluorescent
Screen
electron beam
10 keV (λo=0.124 Å)
λ_o
L
t
$d_{//} \cdot t = L \cdot \lambda_o$

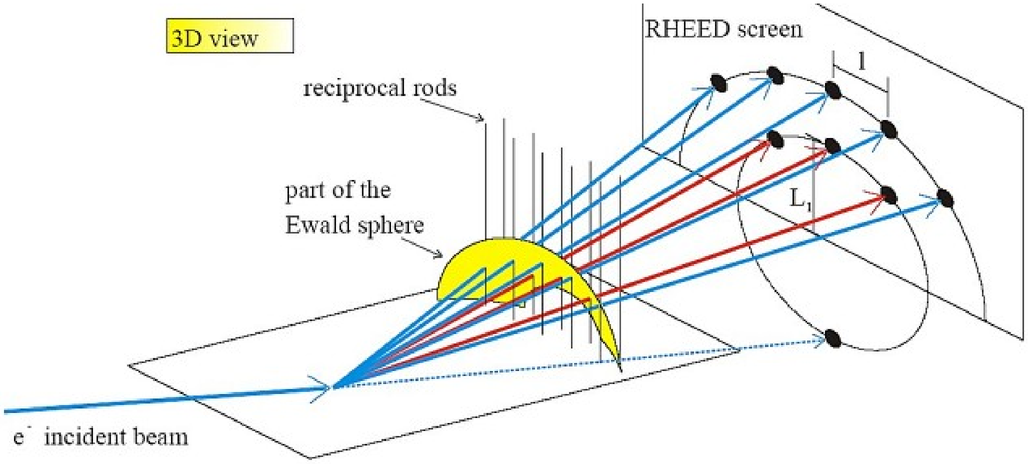

3D view
RHEED screen
reciprocal rods
part of the
Ewald sphere
e⁻ incident beam

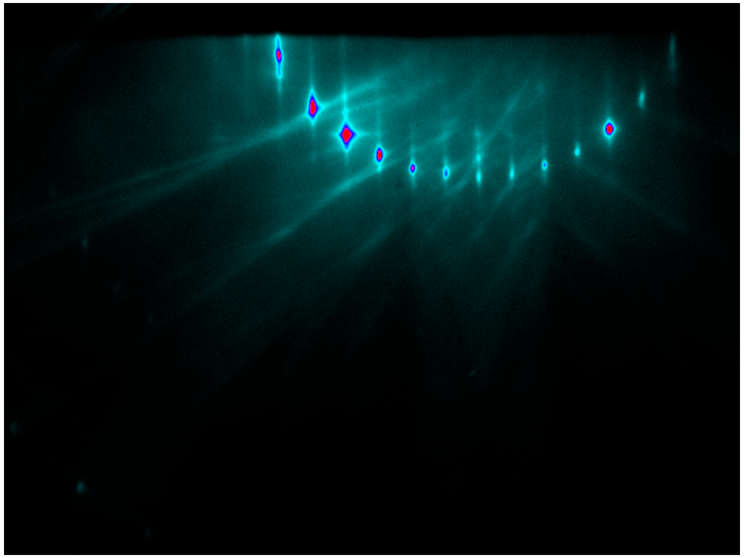

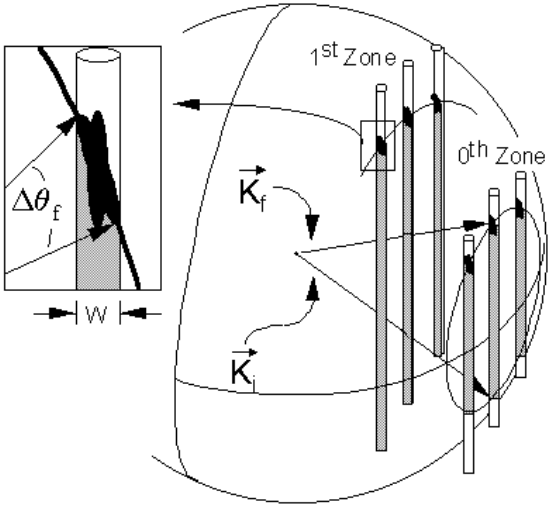

1st Zone
0th Zone
W

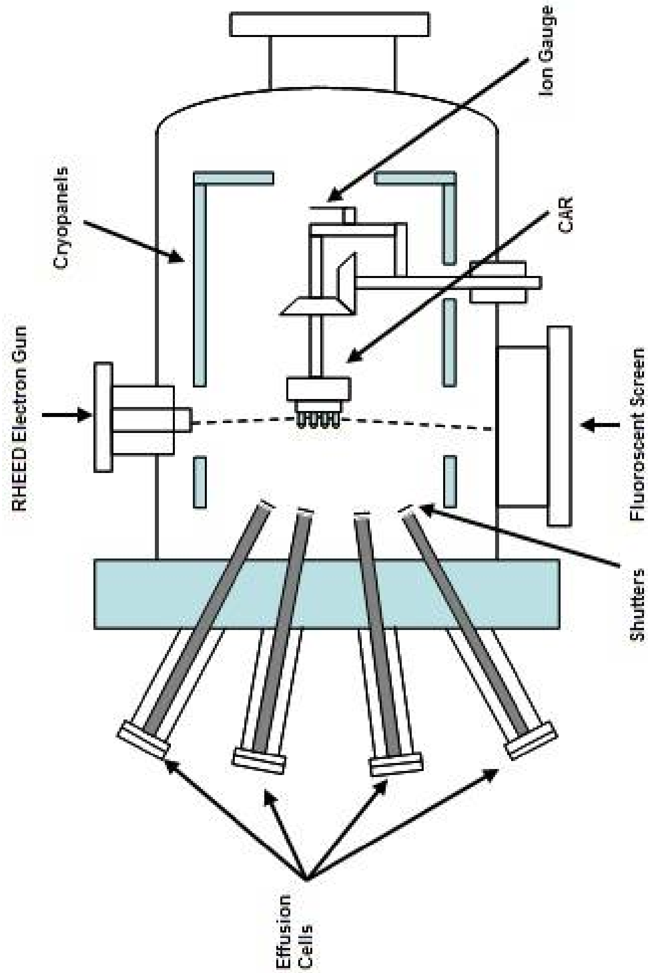
Ion Gauge
CAR
Cryopanels
RHEED Electron Gun
Fluoroscent Screen
Shutters
Effusion Cells

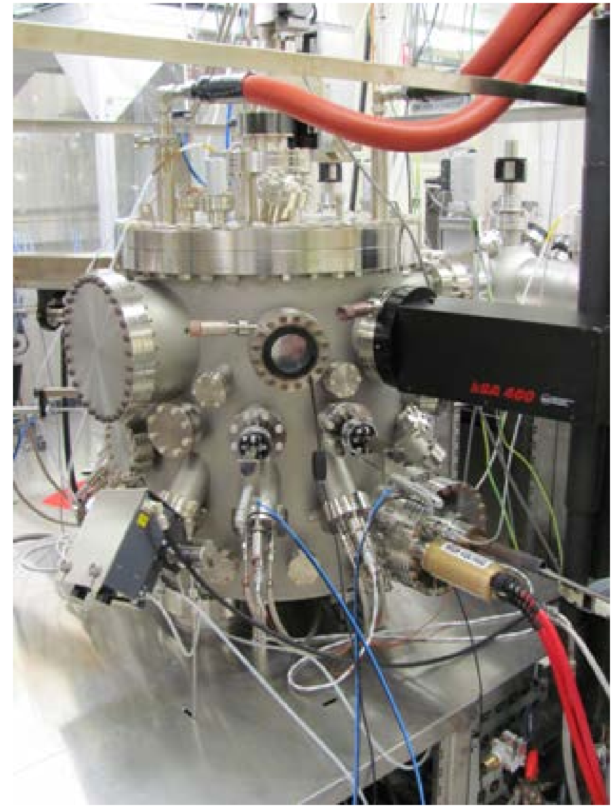

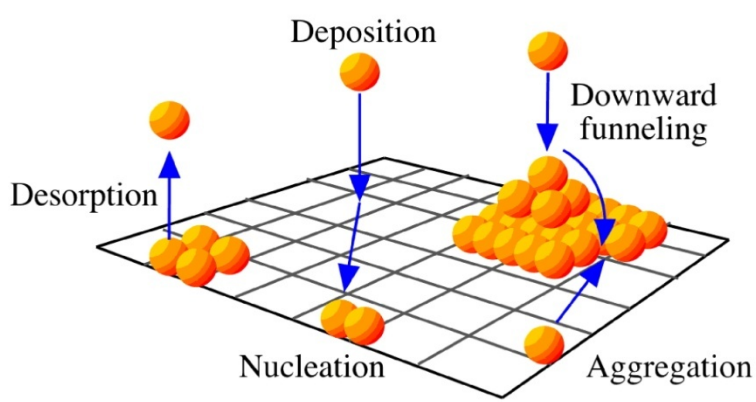
Deposition
Downward funneling
Desorption
Nucleation
Aggregation

Materials Physics Laboratory

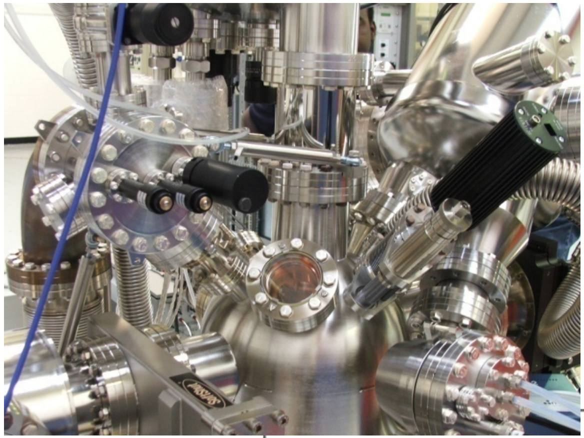

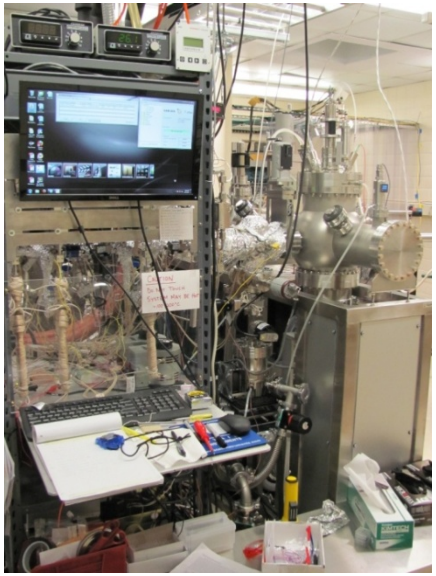

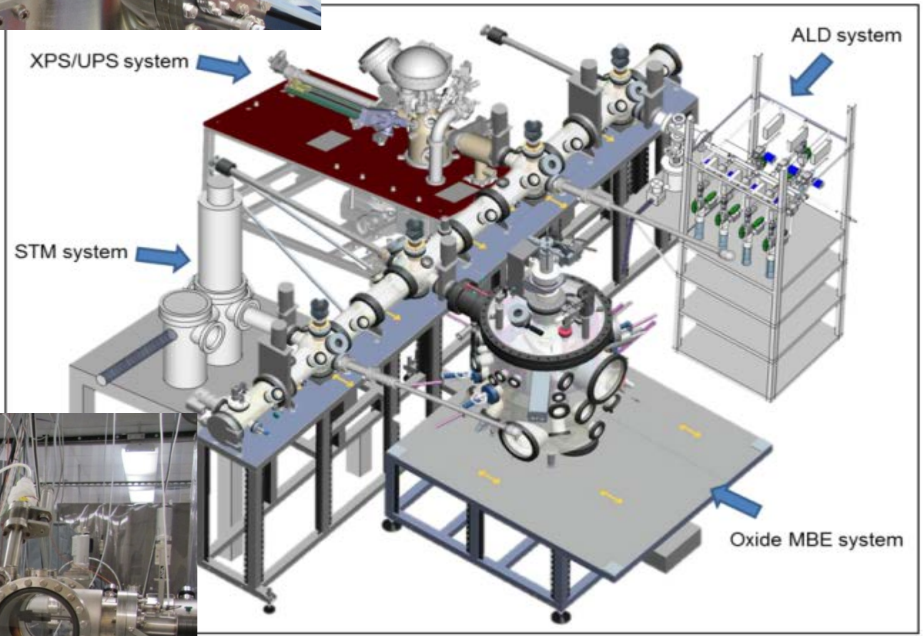

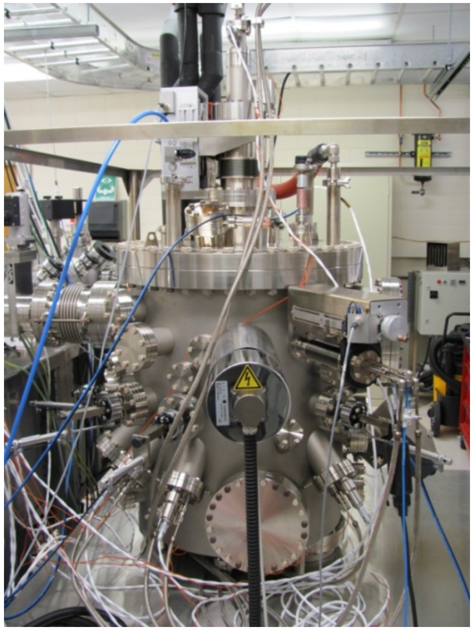

$$\left(-\frac{\hbar^2\nabla^2}{2m}+V(r)\right)\psi_i(r)=\varepsilon_i\psi_i(r)$$

Theoretical methods

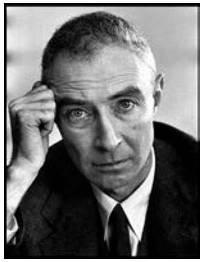

$$\Psi(\mathbf{R},\mathbf{r}) = \sum_{k=1}^{K} \chi_k(\mathbf{r};\mathbf{R})\phi_k(\mathbf{R}),$$

$$H_e\ \chi(\mathbf{r}) = E_e\ \chi(\mathbf{r})$$

$$[T_n + E_e(\mathbf{R})]\,\phi(\mathbf{R}) = E\phi(\mathbf{R})$$

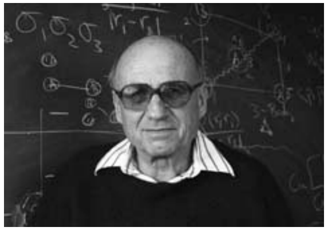

$$E_{KS}[n]=\left\langle \Psi\middle|\hat{H}\middle|\Psi\right\rangle = E_{K.E}[n]+E_{Hartree}[n]+E_{elec-ion}[n]+E_{ion-ion}+E_{XC}[n]$$

$$\left(-\frac{\hbar^2\nabla^2}{2m}+V_{KS}(r)\right)\psi_i(r)=\varepsilon_i\psi_i(r)$$

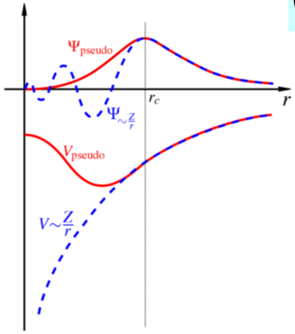

$$V_{KS}(r)=V_{ext}(r)+\int\frac{n(r')}{|r-r'|}dr'+V_{XC}(r)$$

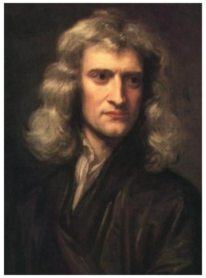

$$F_i=-\frac{\partial E}{\partial R_i}\longrightarrow F_i=m_i\ddot{x}_i$$

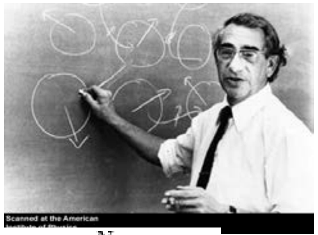

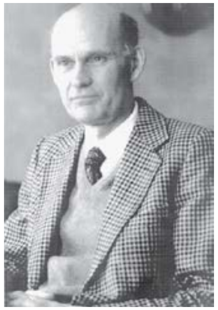

$$H = -t\sum_{<i,j>,\sigma} c^\dagger_{i,\sigma}c_{j,\sigma} + U\sum_{i=1}^{N} n_{i\uparrow}n_{i\downarrow}$$

$$E_i=\varepsilon_i+\left\langle\Phi_i\middle|\Sigma(E_i)-V_{xc}\middle|\Phi_i\right\rangle\approx\varepsilon_i+Z_i\left\langle\Phi_i\middle|\Sigma(\varepsilon_i)-V_{xc}\middle|\Phi_i\right\rangle$$

$SrTiO_3/LaAlO_3$ heterostructure:

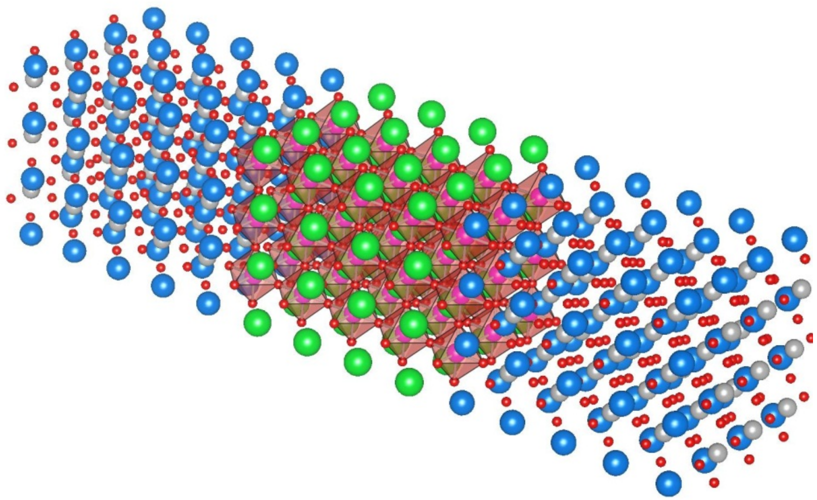

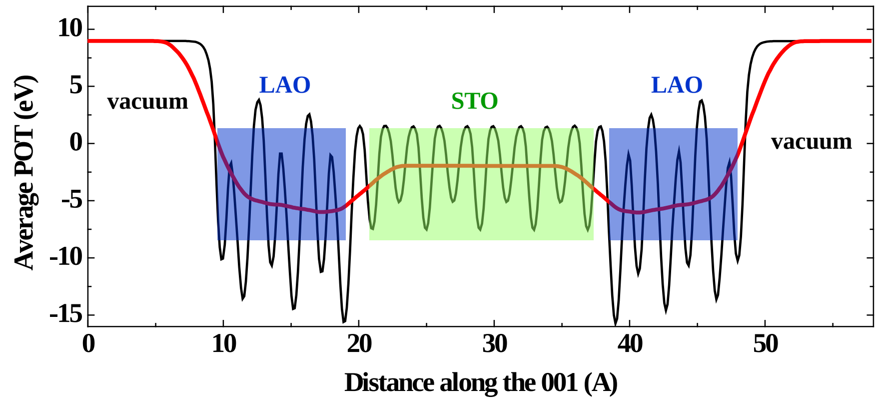

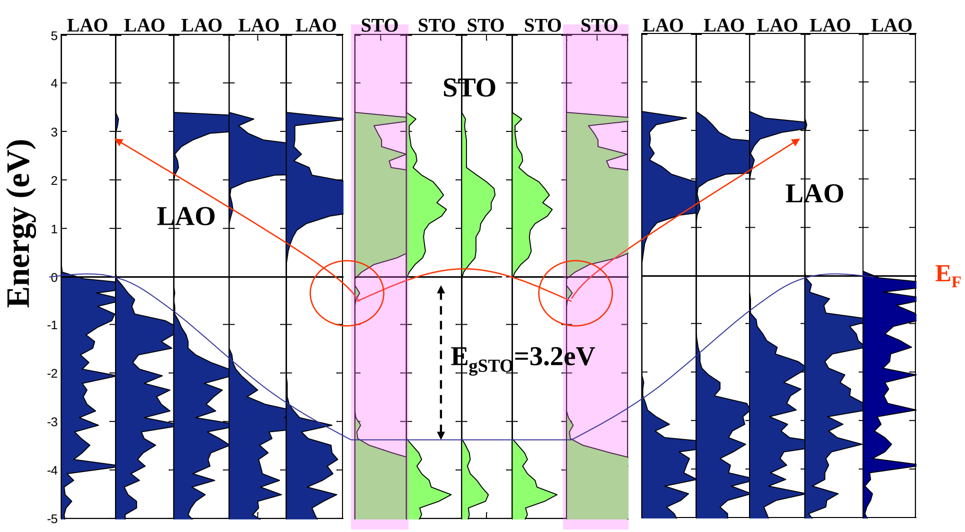

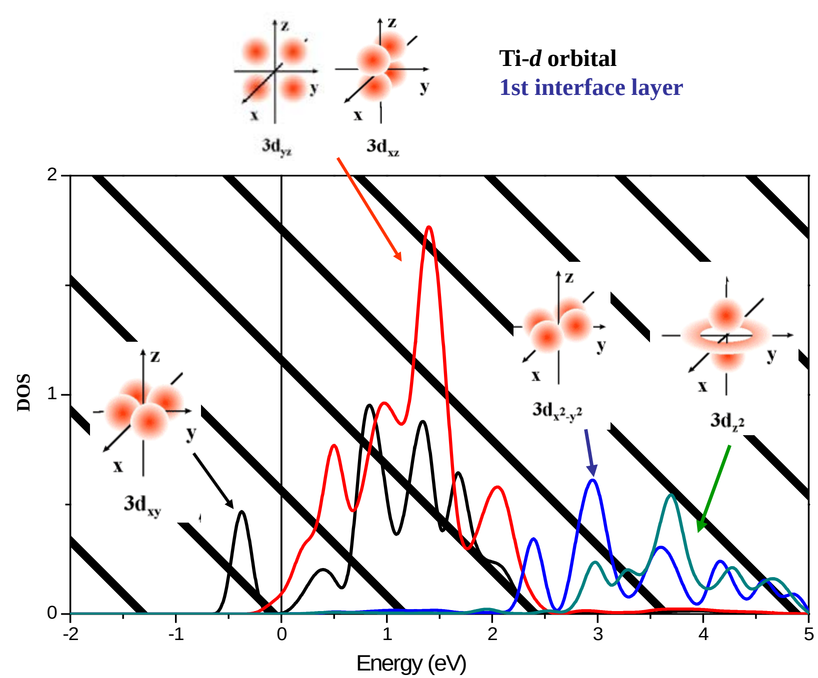

J.K. Lee and AAD, Phys. Rev. B **78**, 146839 (2008)

COX: Crystalline oxide on semiconductor

$SrTiO_3$ on Si

Model | **Experiment**

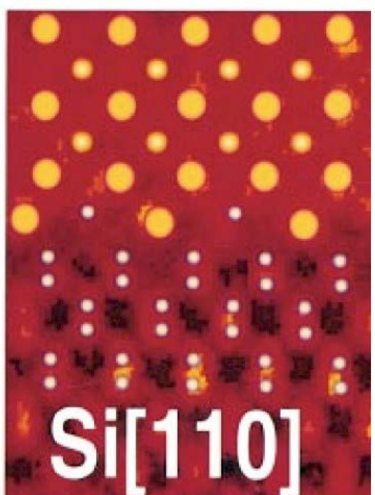

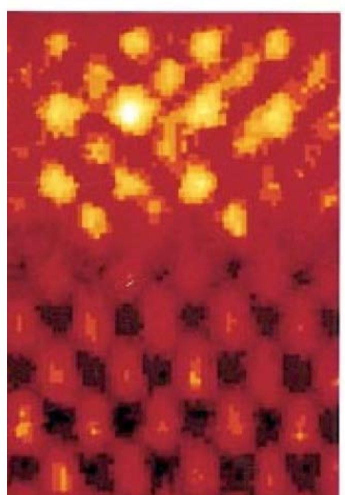

$BaTiO_3$ on Ge

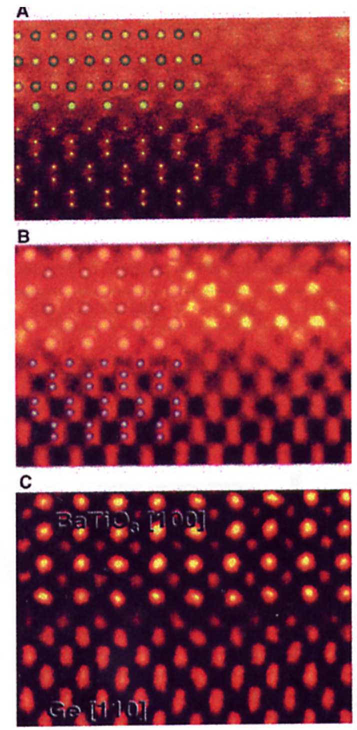

Fig. 1. Alkaline earth and perovskite oxide heteroepitaxy on silicon and germanium. The figure illustrates our ability to manipulate interface structure at the atomic level using our $(AO)_n(A'BO_3)_m$ structure series. The n/m ratio defines the electrical characteristics of this new physical system of COS in a MOS capacitor. In (**A**), $n = 3, m = 0$; in (**B**), $n = 1, m = 2$; in (**C**), $n = 0, m = 3$.

R. McKee, F. Walker, M. Chisholm, *PRL* 81 3014 (1998)
R. McKee, F. Walker, M. Chisholm, *Science 293, 468 (2001)*

Si and STO are very different!

A. Geometry:

Silicon

45 ° “rotation”

ABO_3

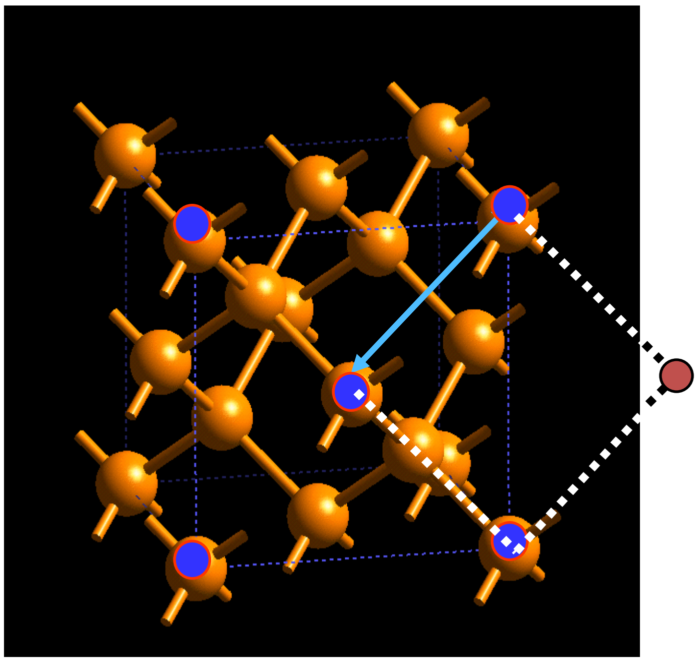

A-layer

B-layer

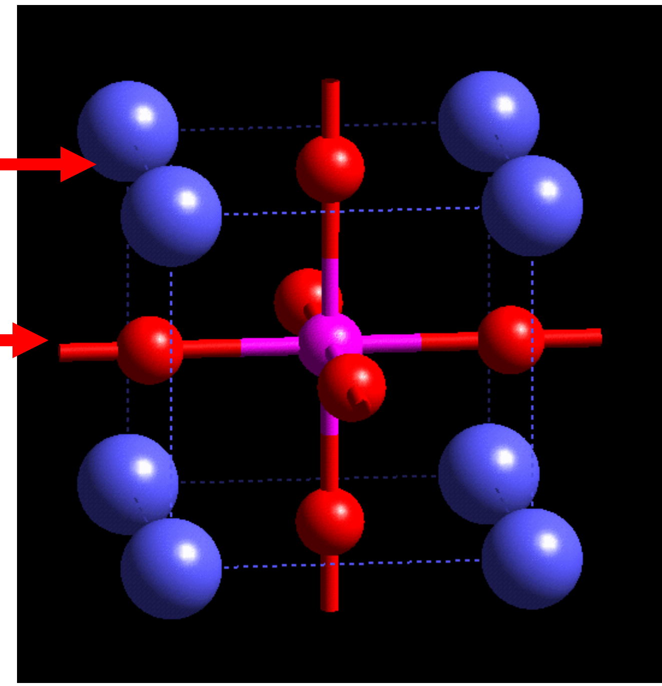

$a_{Si}/(2)^{0.5}=3.84$ Å

$a_{STO}=3.905$ Å

B. Chemistry:

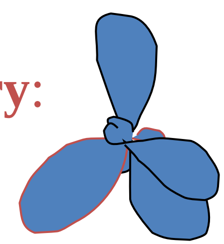

?

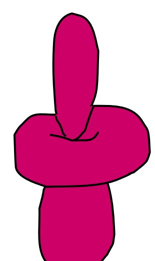

Zintl intermetallics : $SrAl_2$

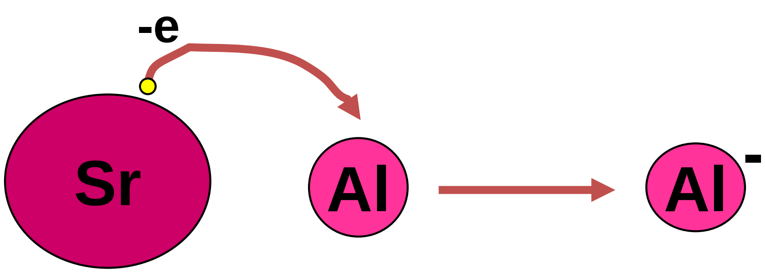

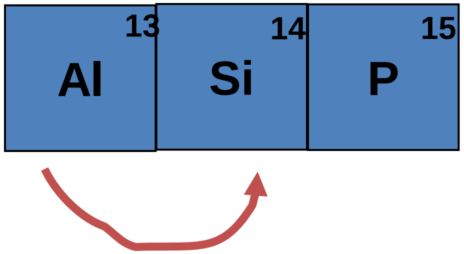

Zintl Alchemy

Edward Zintl (1898-1941)

fcc Al metal

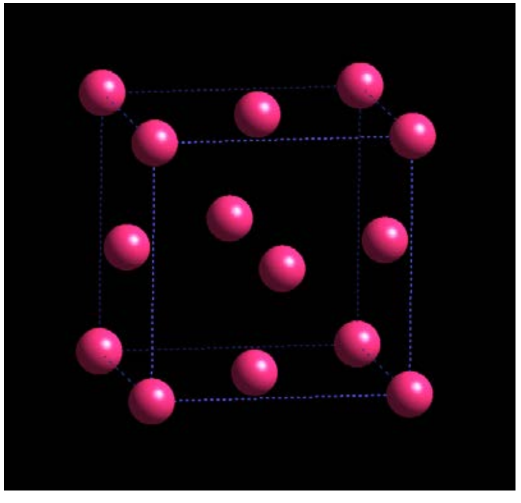

$SrAl_2$ structure

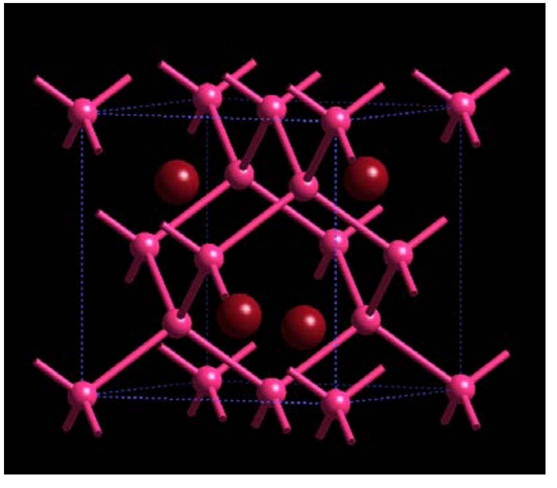

tI10 $SrAl_4$ structure

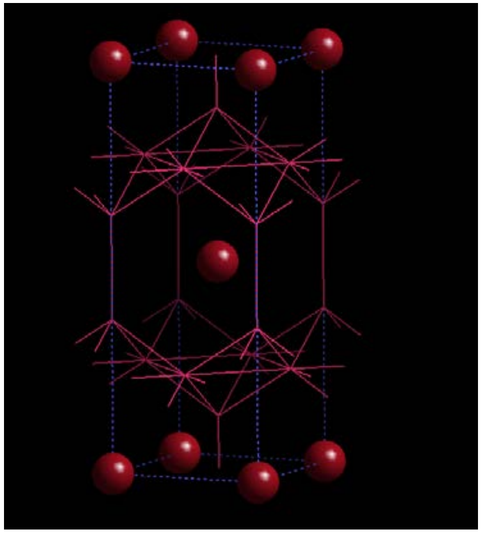

$SrTiO_3$ deposition on Si

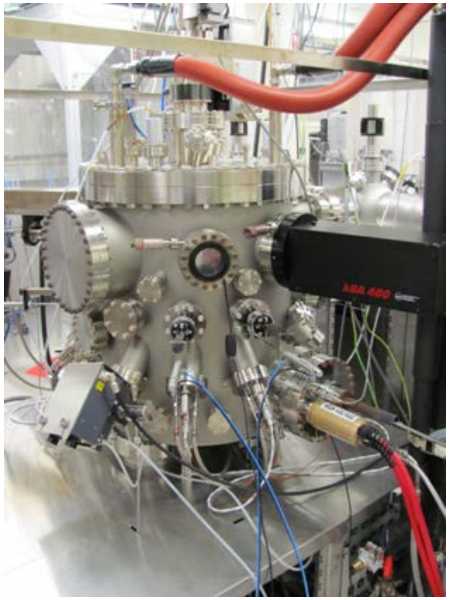

- Sr-assisted SiO_2 desorption

Y. Wei et al., J. Vac. Sci. Technol. B **20**, 1402 (2002).

B. K. Moon and H. Ishiwara, Jpn. J. Appl. Phys., Part 2 **33**, L472 (1994).

- ½ monolayer Sr on Si

  (Zintl template layer)

Edward Zintl
1898-1941

- Initial amorphous $SrTiO_3$ seed layer at 200°C (4 unit cells)
  - Crystallize at 550°C
- Main $SrTiO_3$ deposition
  - $4x10^{-7}$ torr O_2 at 550°C
  - Co-evaporation of Sr and Ti at 1 monolayer per minute
  - 20 unit cells (fully relaxed)

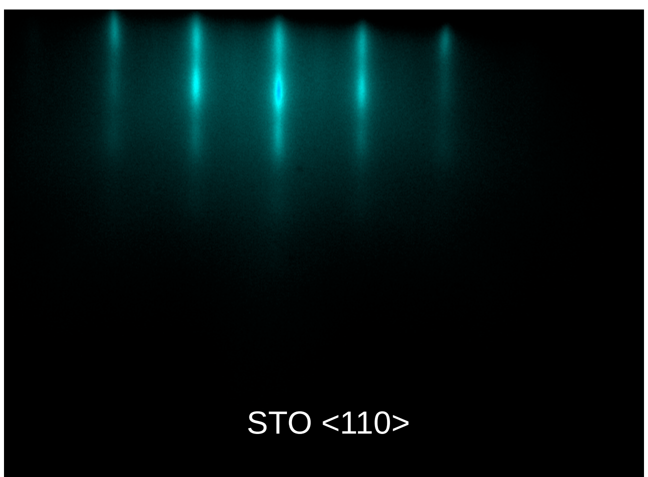

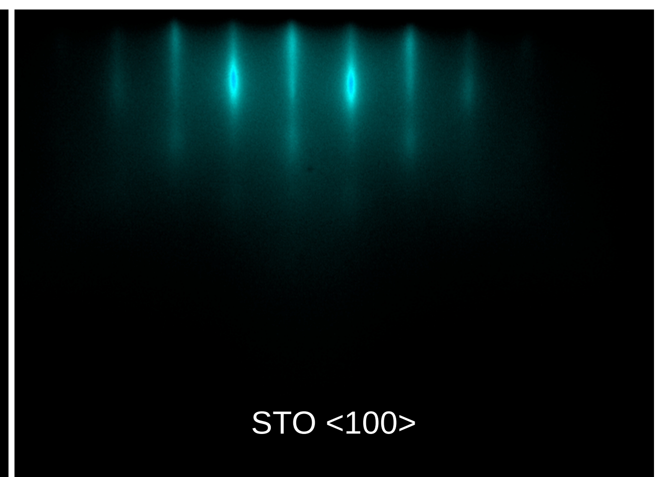

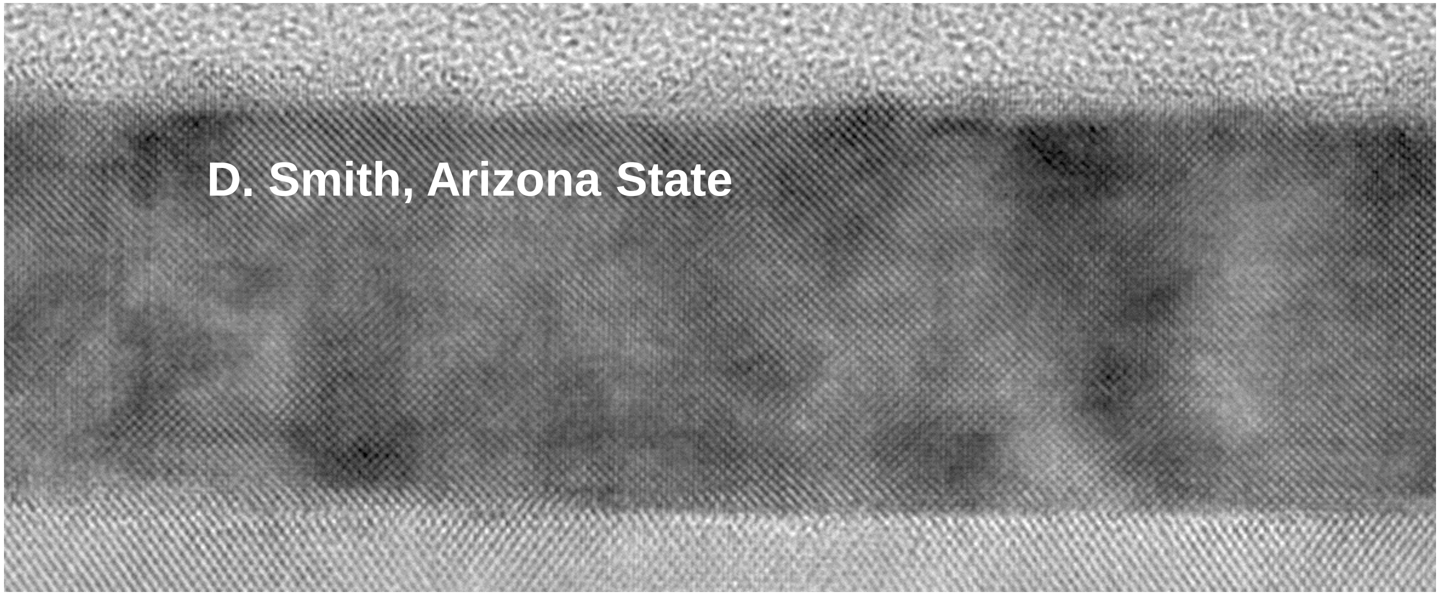
D. Smith, Arizona State

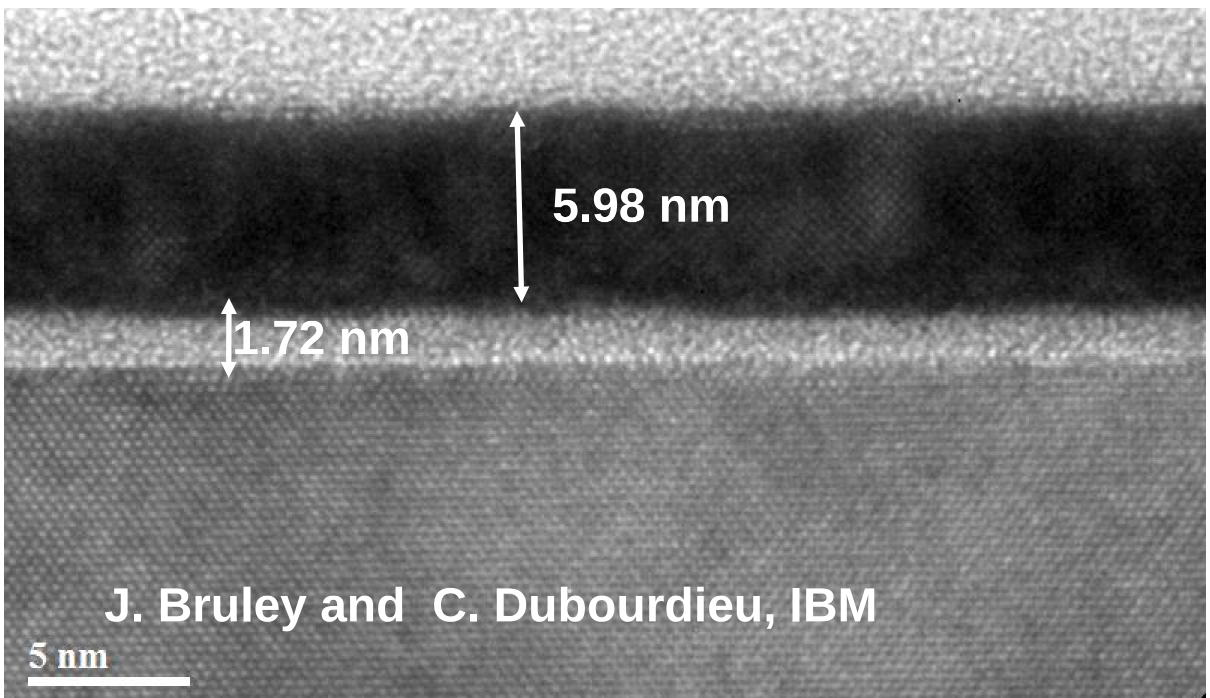
5.98 nm
1.72 nm
J. Bruley and C. Dubourdieu, IBM
5 nm

Integrating ferromagnets on Si (001)

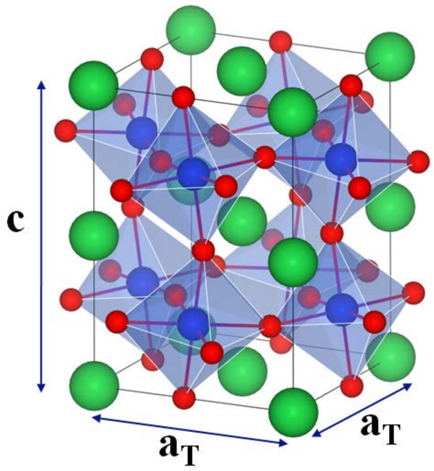

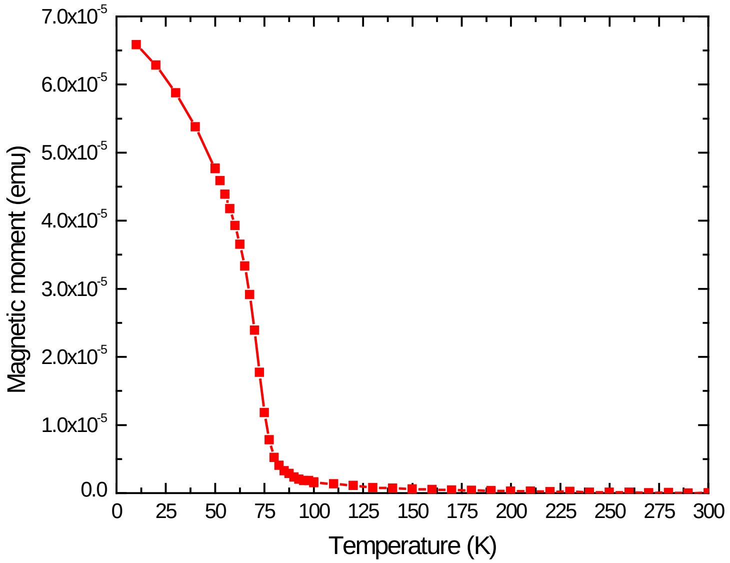

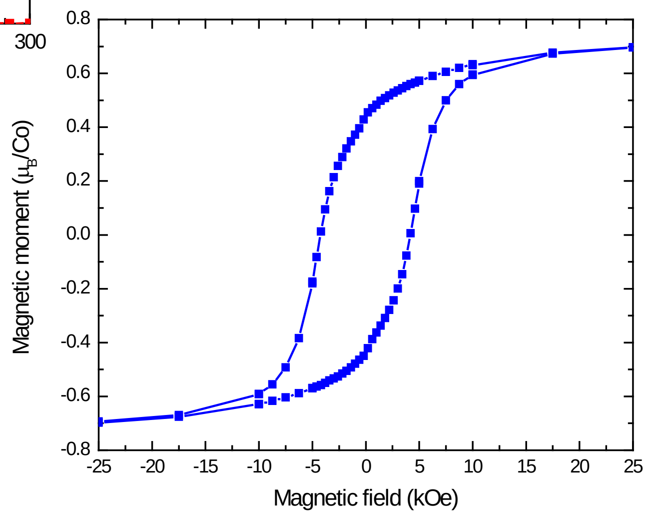

Properties and applications $La_{1-x}Sr_xCoO_3$

- Properties
  - Co^{3+} : $3d^6$
  - 0.6 eV gap semiconductor
  - Non-magnetic at low temperature but paramagnetic at room temperature
  - **Epitaxial strain induces ferromagnetism***
  - Spin state transitions
    - Low, intermediate, high-spin
  - Metal-insulator transition when doped
- Possible applications
  - Electrode (Sr-doped)
    - Cathode material for solid oxide fuel cells
    - Epitaxial oxide electrode for perovskite multilayers
  - Gas sensors / catalysis
  - Magnetic semiconductor
    - Spintronics

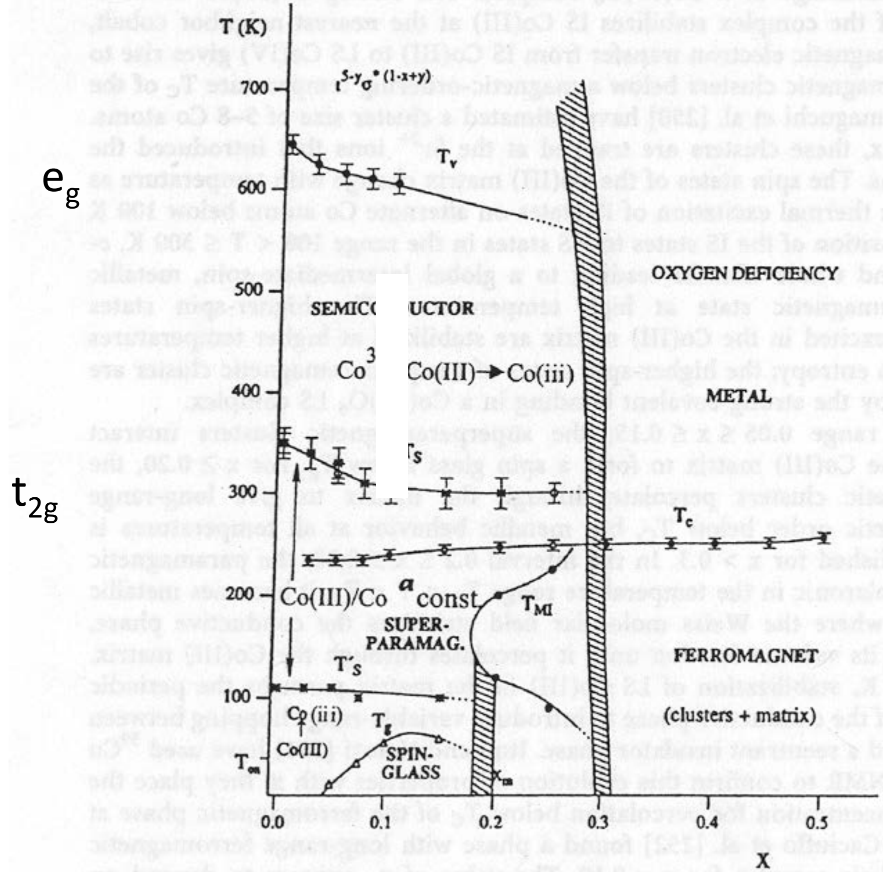

Fig. 41. Phase diagram of $La_{1-x}Sr_xCoO_3$ ($0 = x = 0.50$); adapted from [247]. Co(III) = low-spin; Co(iii) = intermediate-spin; Co^{3+} = high-spin

- **Fuchs et al., PRB 75, 144402 (2007)**
- **Rondinelli&Spaldin, PRB 79, 054409 (2009) NO**
- **Gupta&Mahadevan, PRB 79, 020406 (2009) YES**

$LaCoO_3$

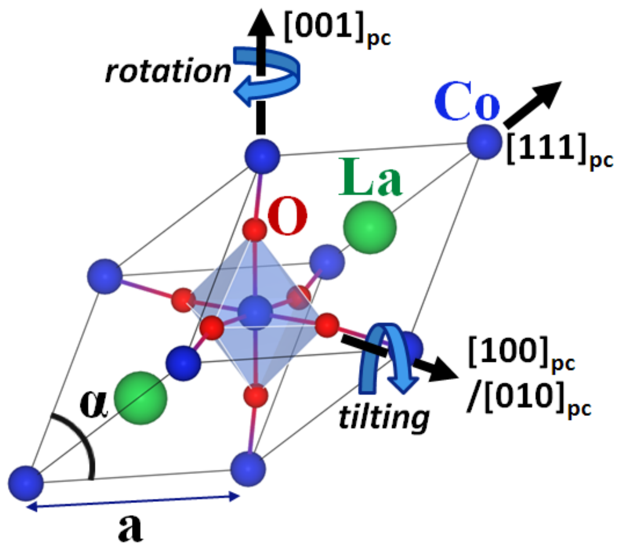

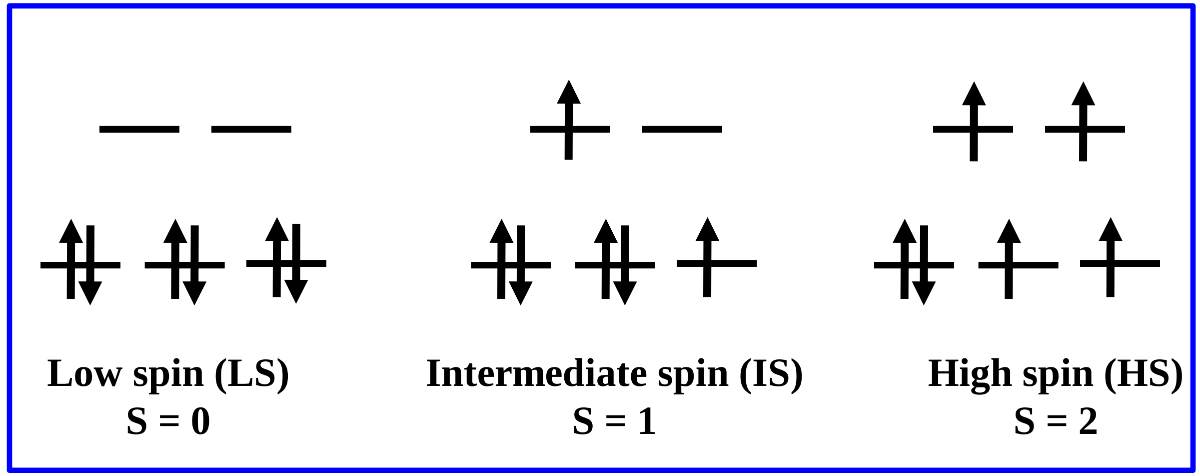

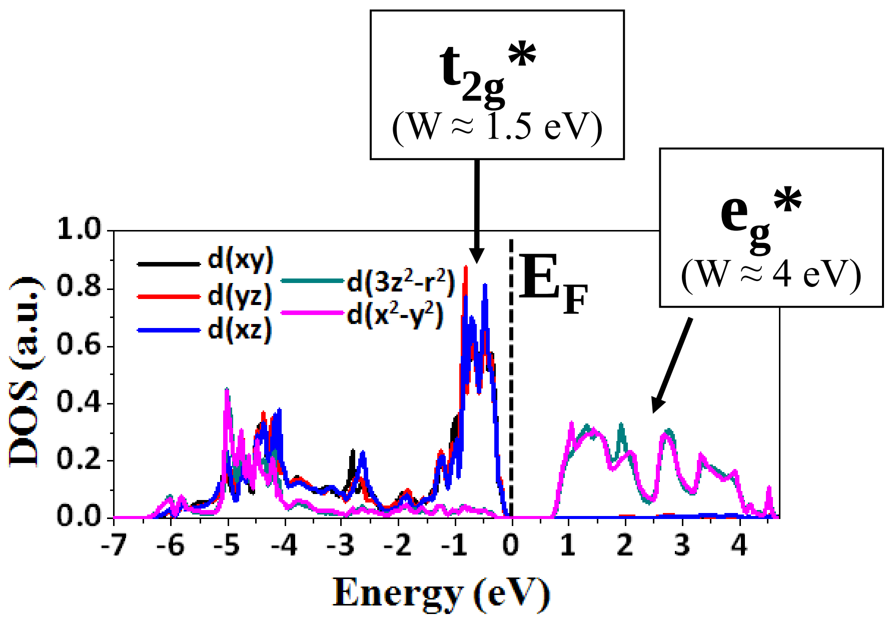

*Low spin (LS); S = 0

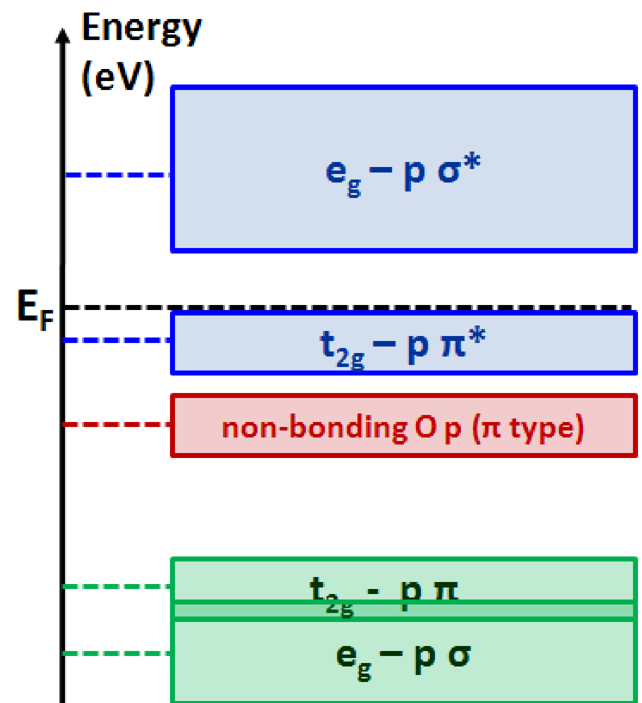

Energy vs. strain

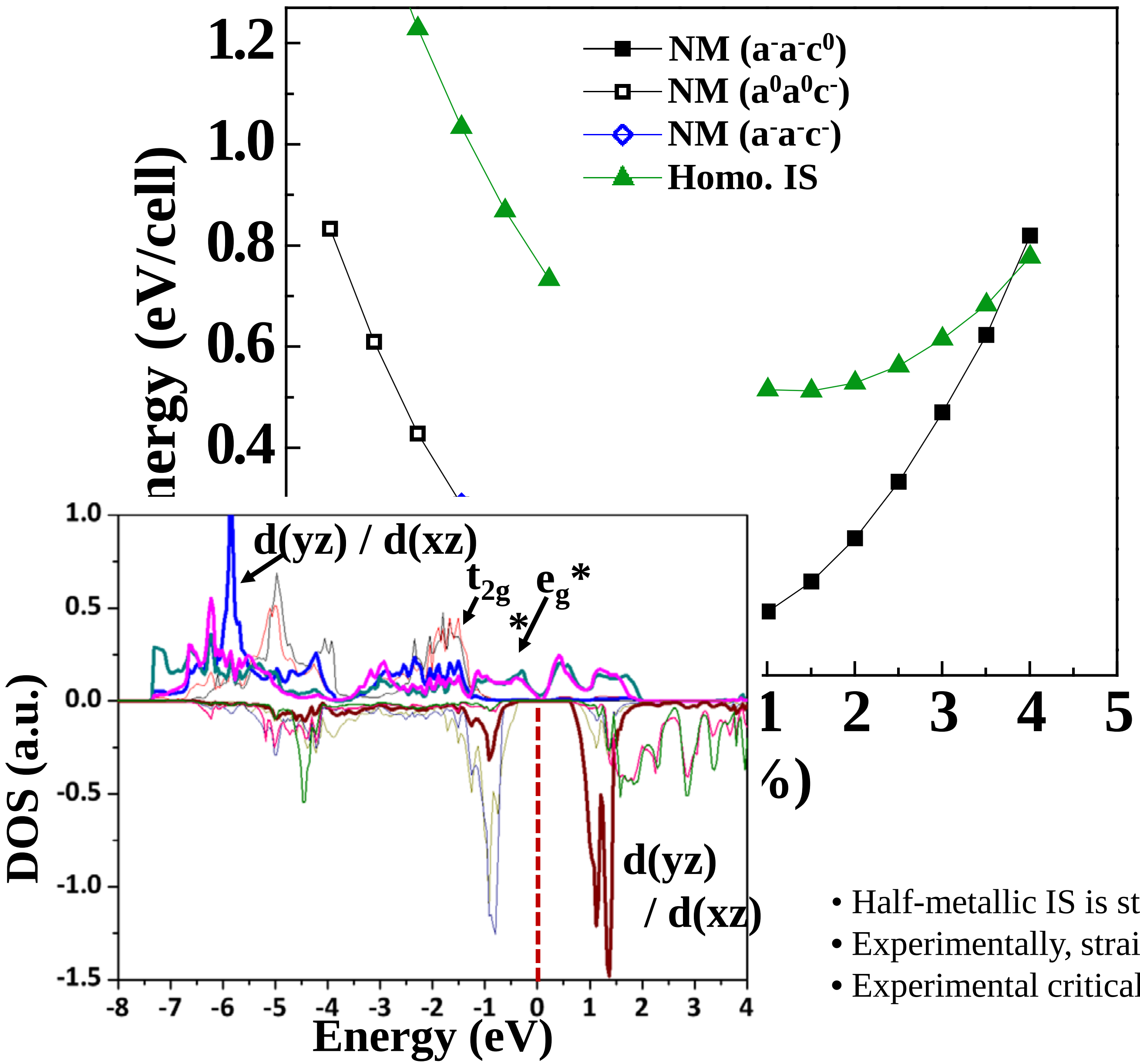

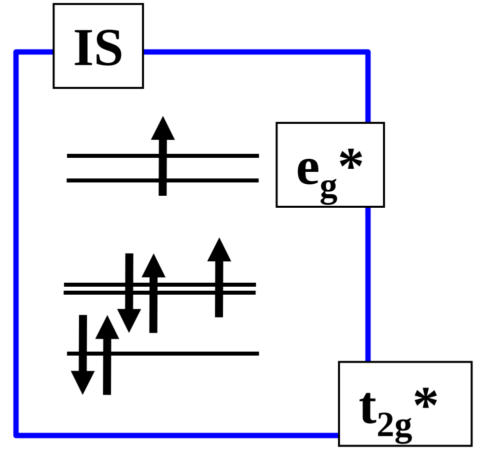

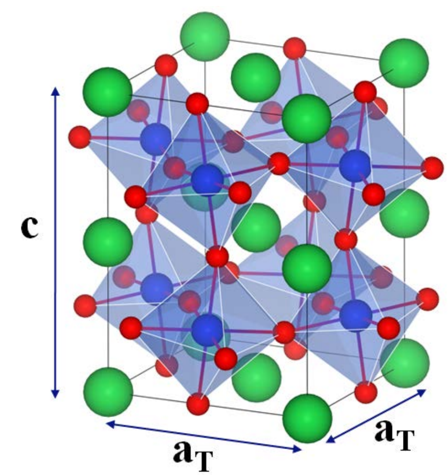

- Half-metallic IS is stabilized beyond 3.8%.
- Experimentally, strained LCO on STO is insulating.
- Experimental critical strain is less than 3.8%.

Issues related to MBE growth of LCO on Si

- Direct deposition of La, Co on Si in oxygen at high temperature will form $CoSi_2$ and SiO_2
  - Incommensurate or amorphous → Prevents epitaxy
- Phase formation range of $LaCoO_3$ requires both high oxygen chemical potential and high temperature
  - Typical MBE growth conditions using molecular oxygen (10^{-6} torr) results in Co^{2+} oxidation state
- **To overcome these difficulties we will use an $SrTiO_3$/Si pseudo substrate**
  - Use an epitaxial template layer → $SrTiO_3$ on Si
  - Use activated oxygen → atomic oxygen from rf plasma source

Growth of $LaCoO_3$ on STO/silicon

- Atomic oxygen
  - 300 W rf power
  - $1x10^{-5}$ torr background oxygen pressure
- Substrate temperature 750°C
- Co-deposition of La and Co with matched fluxes
  - 2 unit cells per minute rate
- Slow cooling in oxygen
  - 10°C per minute to 100°C

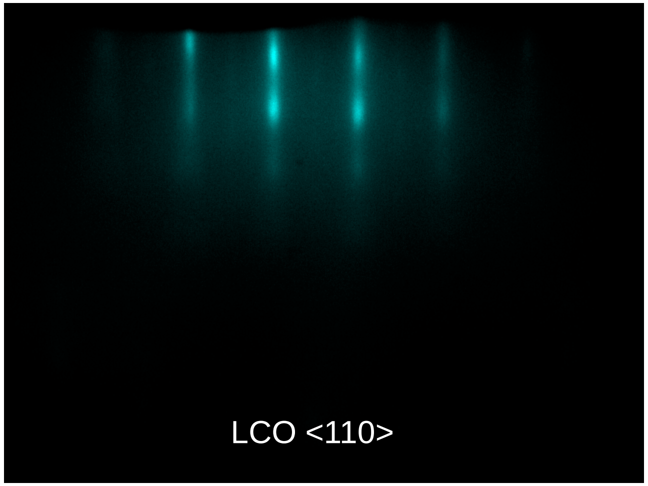

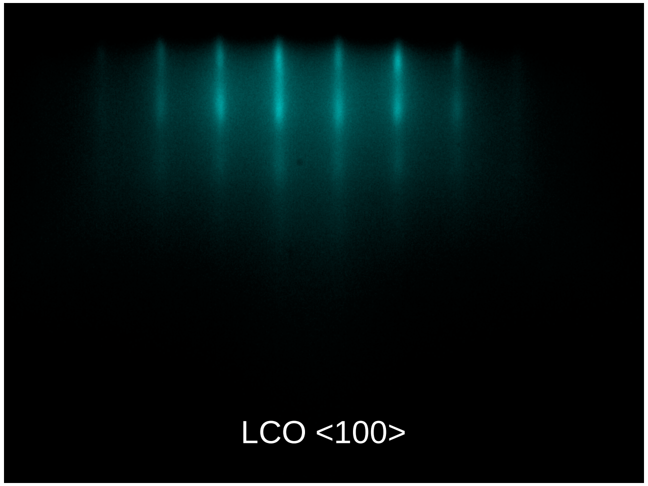

Cross-section TEM

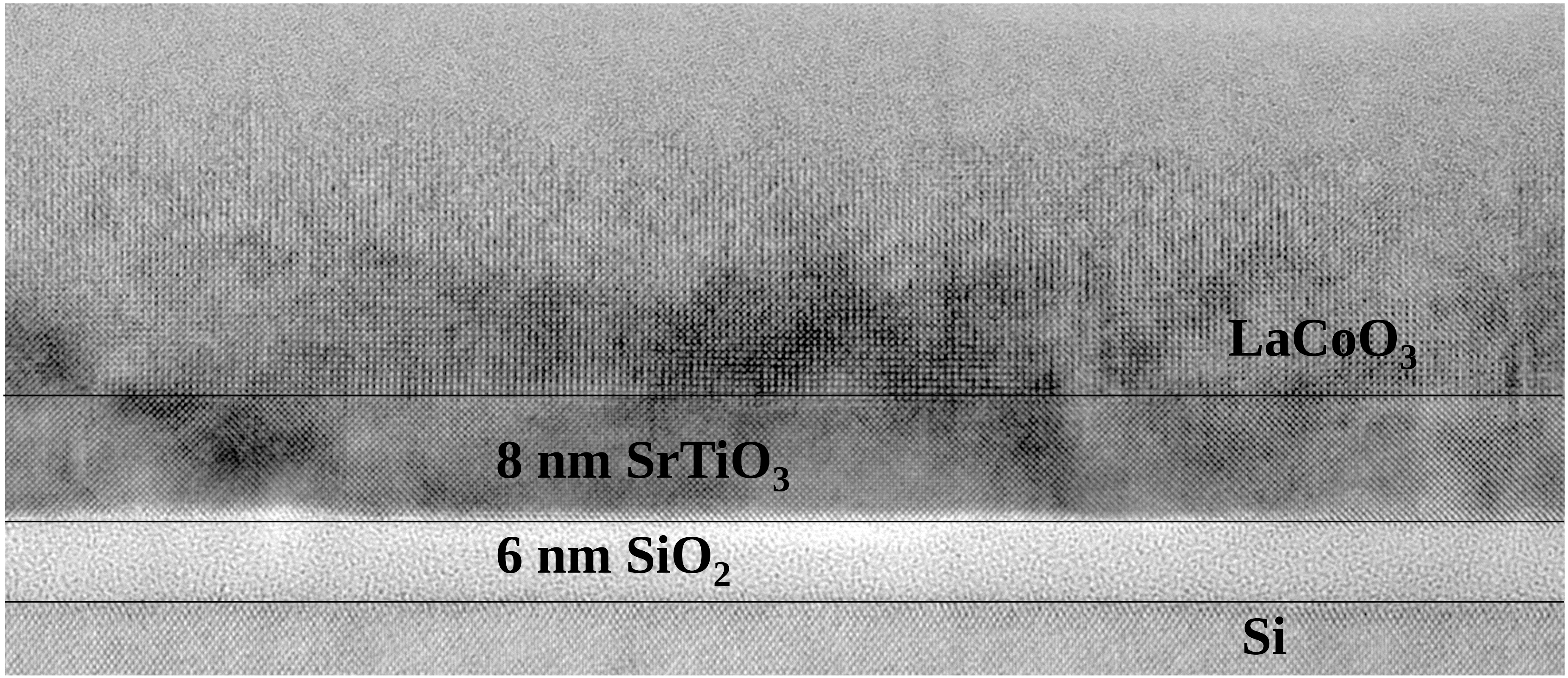

X-ray diffraction

30 nm LCO/8 nm STO/Si

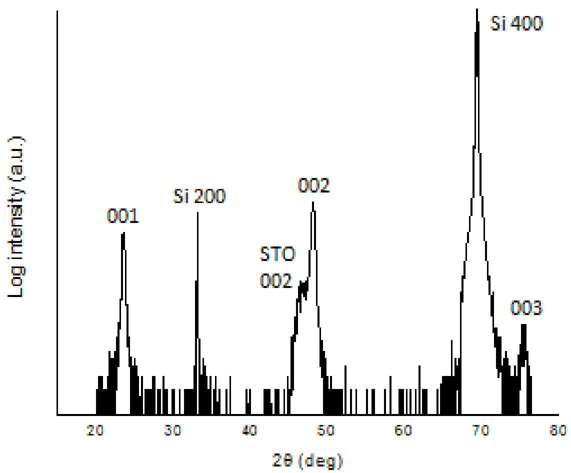

No secondary phases ($La_4Co_3O_{10}$,La_2CoO_4, CoO)

$LaCoO_3$ lattice parameters
(bulk a = 3.80 Å)
c = 3.77 Å
a = 3.89 Å ⟵ Strained to $SrTiO_3$ (a = 3.90 Å)

Core level spectra (XPS)

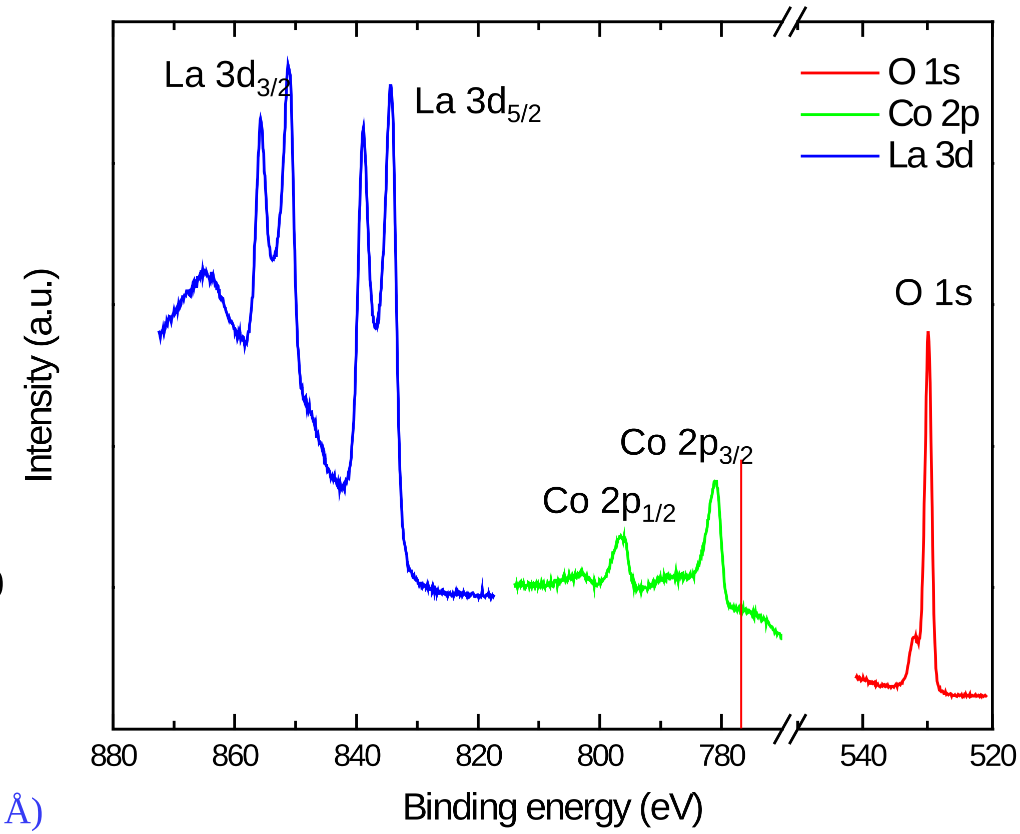

No Co metal detected in XPS
Spectra consistent with literature data for single crystal

Magnetization vs. temperature

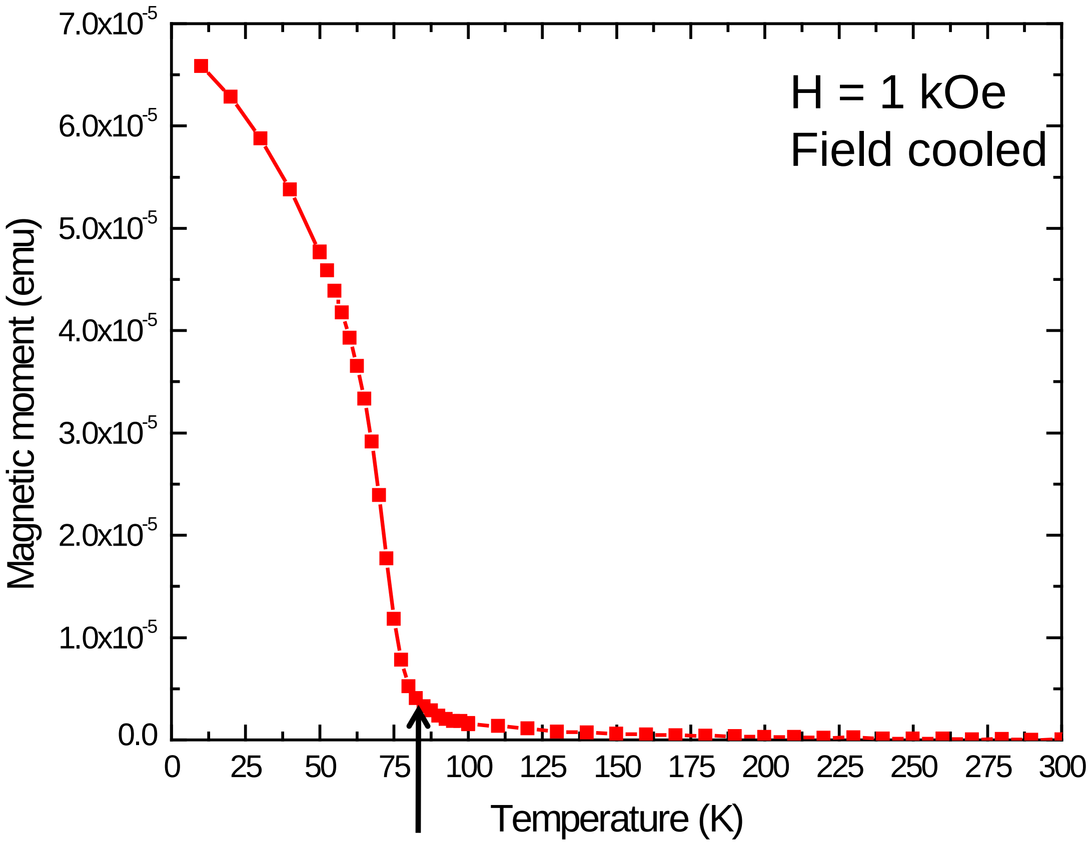

T_C = 85 K

Magnetization vs. field

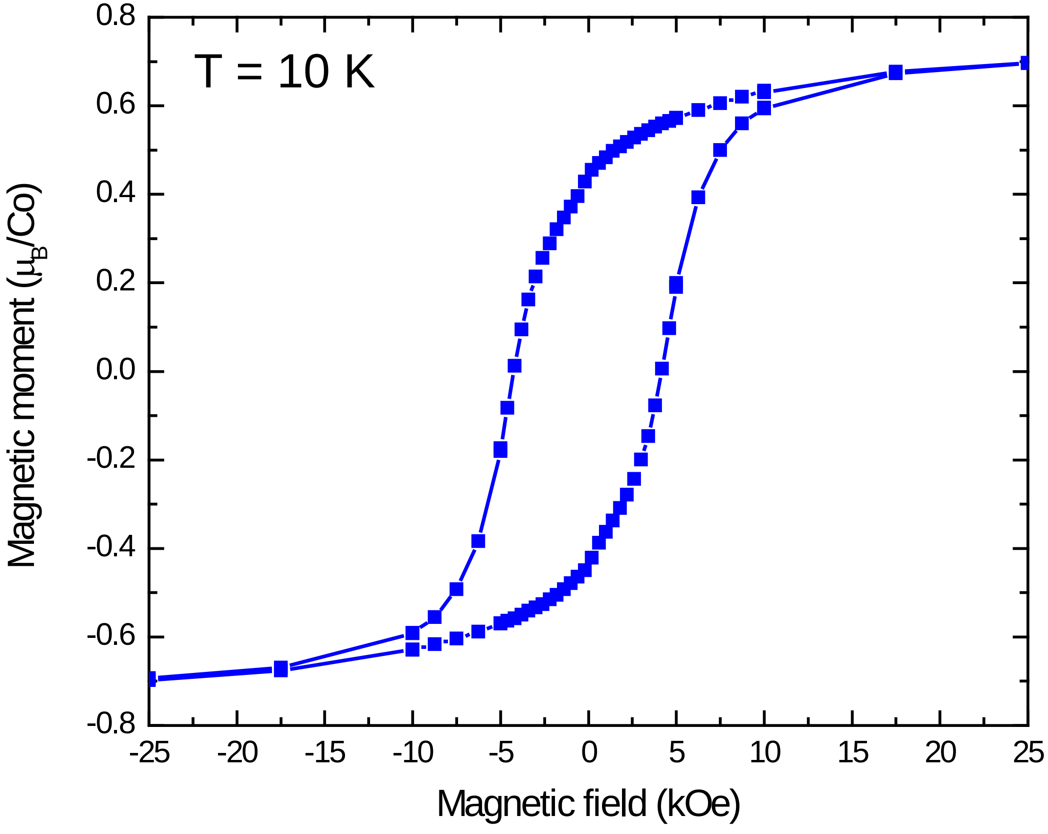

Posadas, et al., Appl. Phys. Lett. **98**, 053104, (2011).

Energy vs. strain

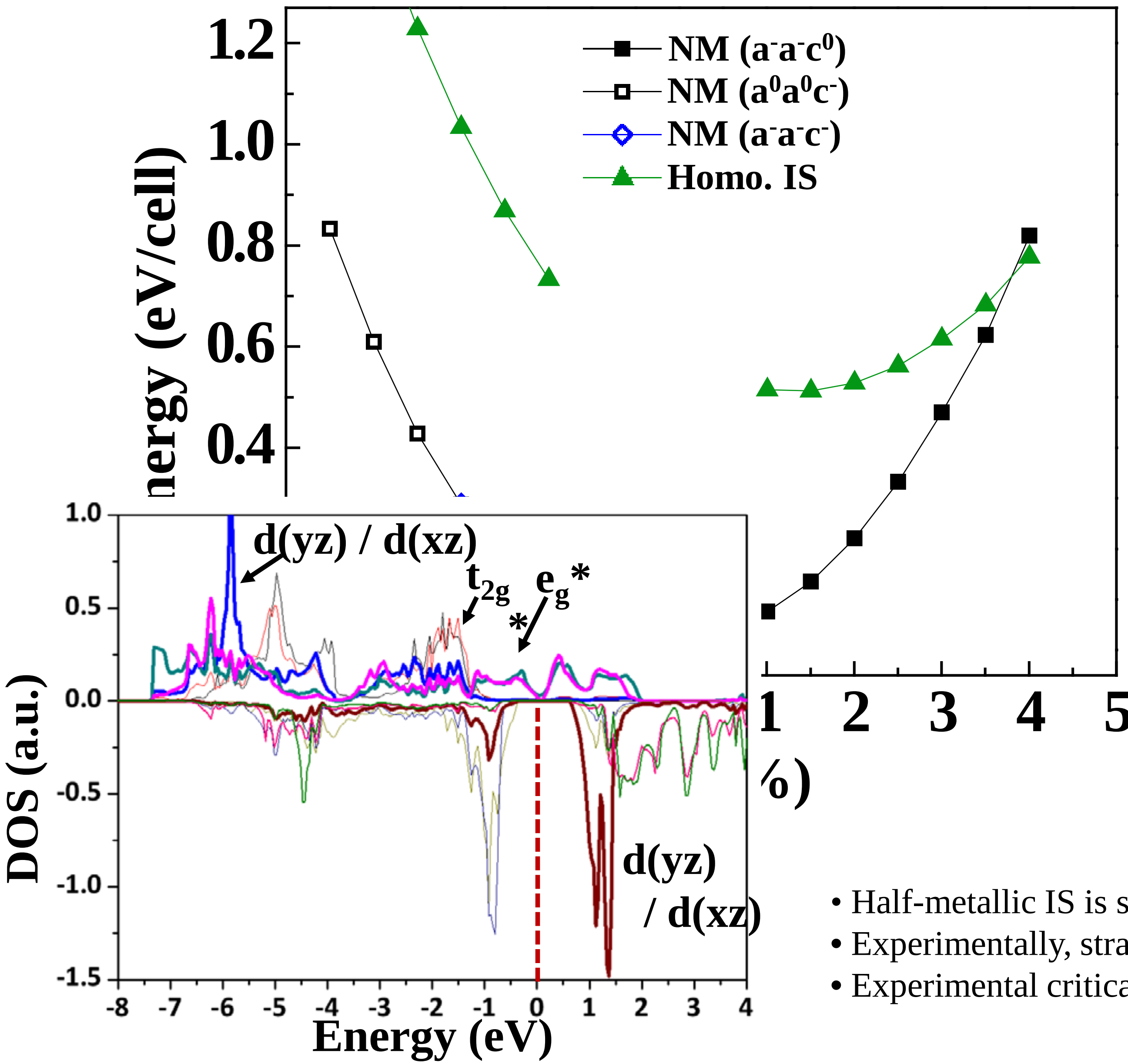

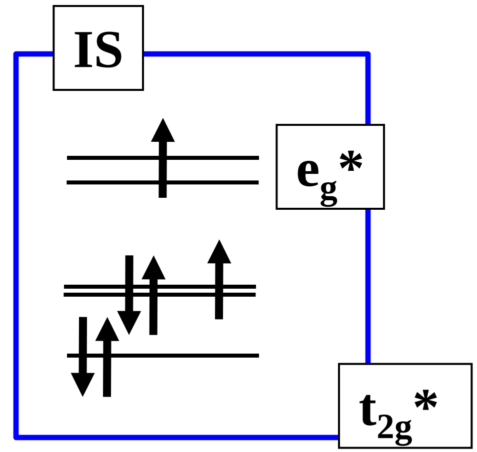

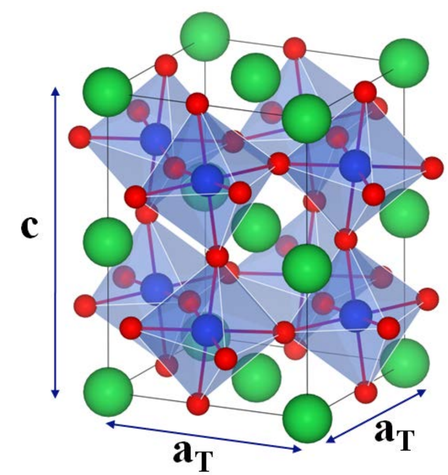

- Half-metallic IS is stabilized beyond 3.8%.
- Experimentally, strained LCO on STO is insulating.
- Experimental critical strain is less than 3.8%.

Supercells

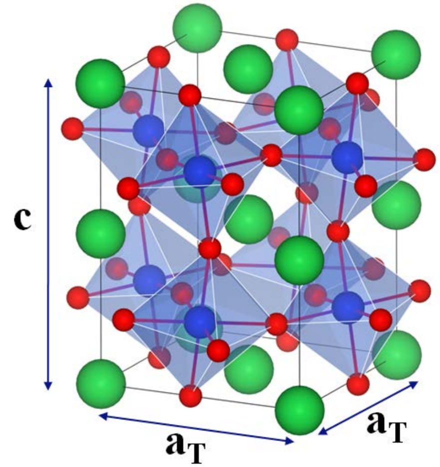

$\sqrt{2}\times\sqrt{2}\times 2$

- 4 independent Co sites
2 in-plane, 2 out-of-plane

$\sqrt{2}\times\sqrt{2}\times 4$

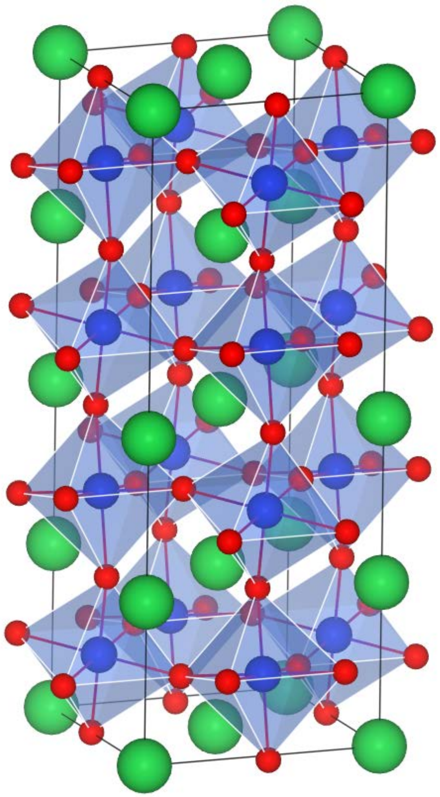

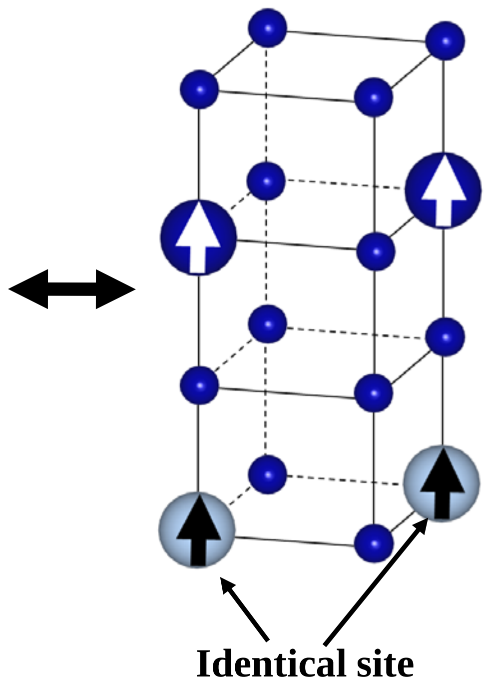

- 8 independent Co sites
2 in-plane, 4 out-of-plane

$2\times 2\times 2$

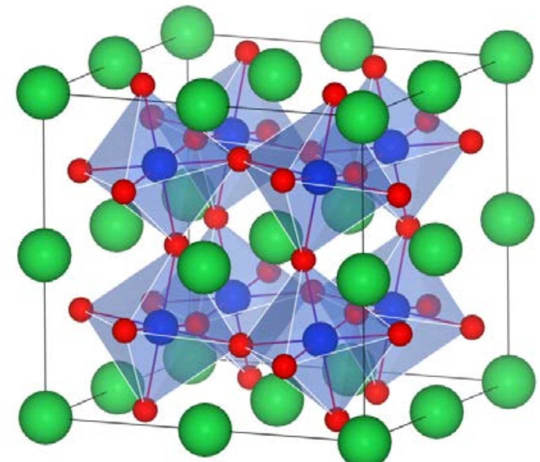

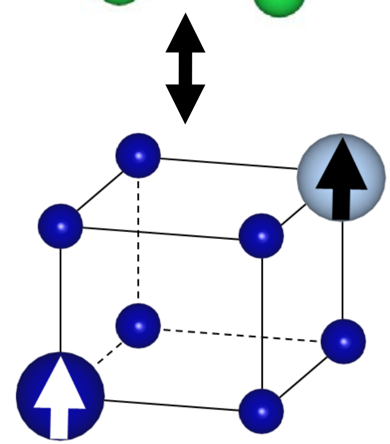

- 8 independent Co sites
4 in-plane, 2 out-of-plane

Energy vs. strain: HS/LS mixed states

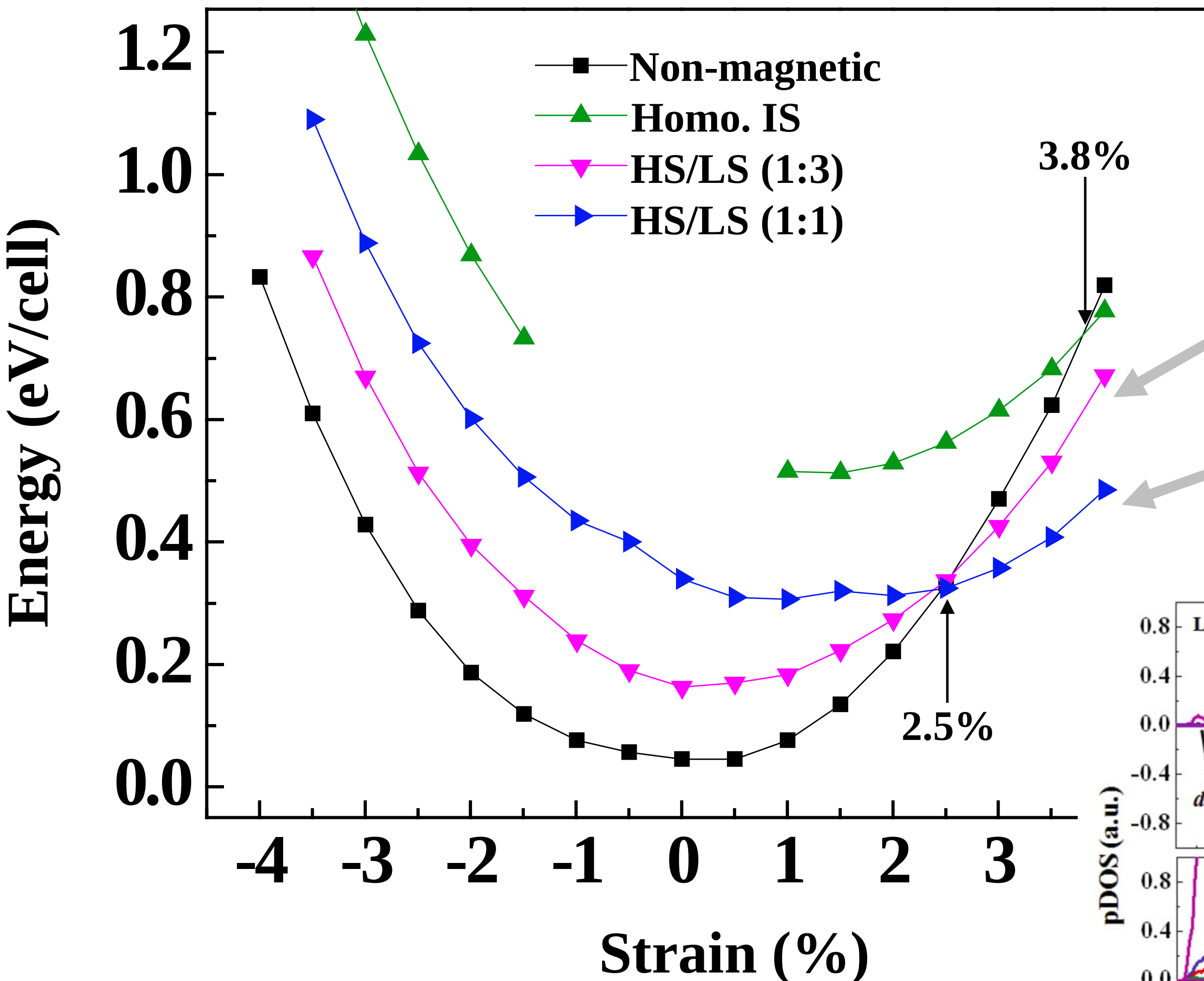

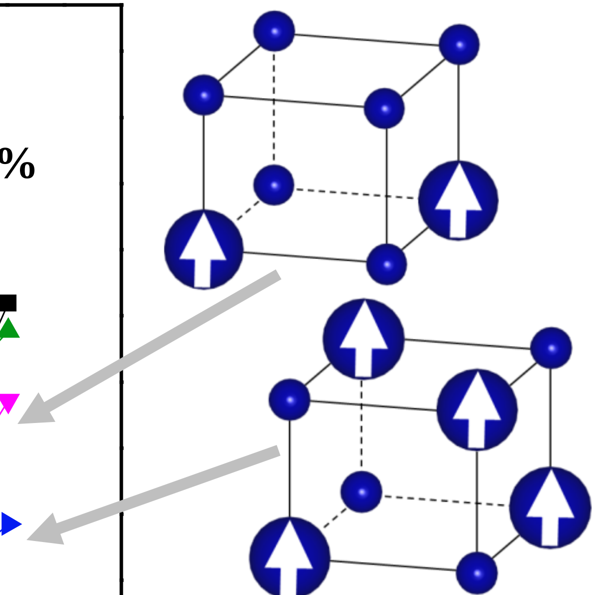

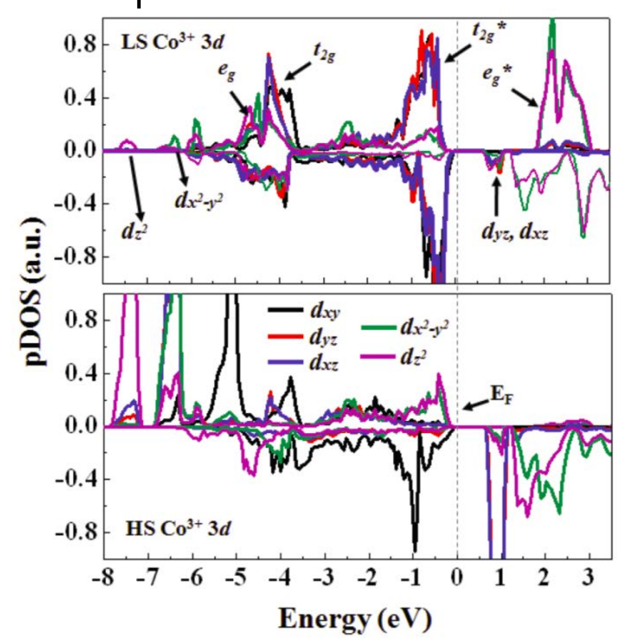

Seo, et al., Phys. Rev. B **86**, 014430 (2012).

Band gap change as a function of strain

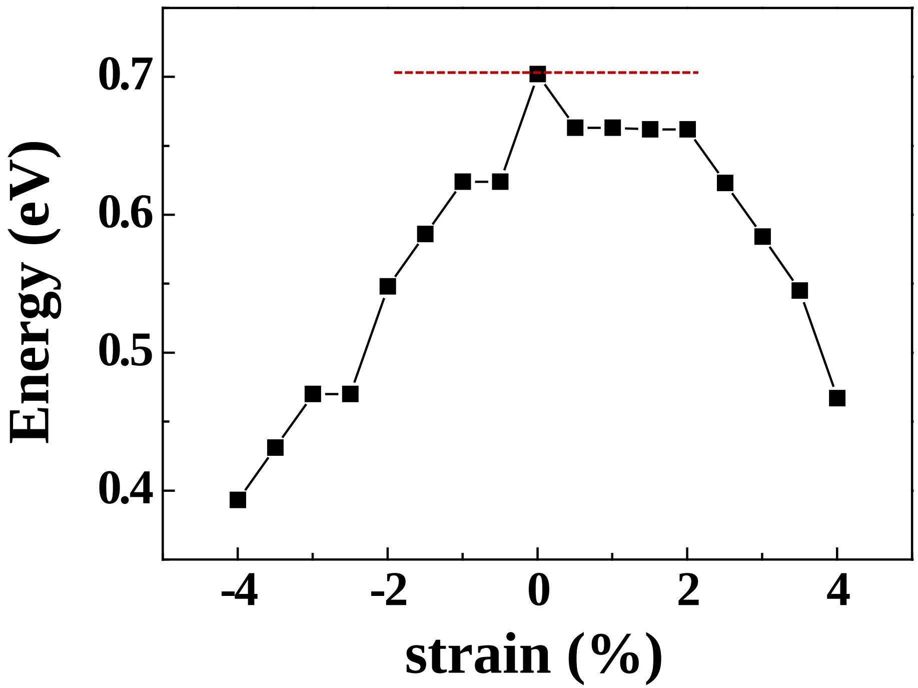

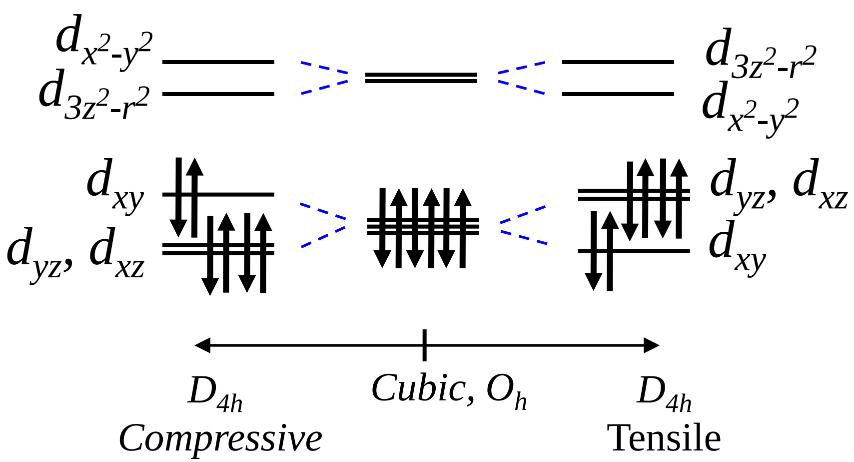

Strain accommodation

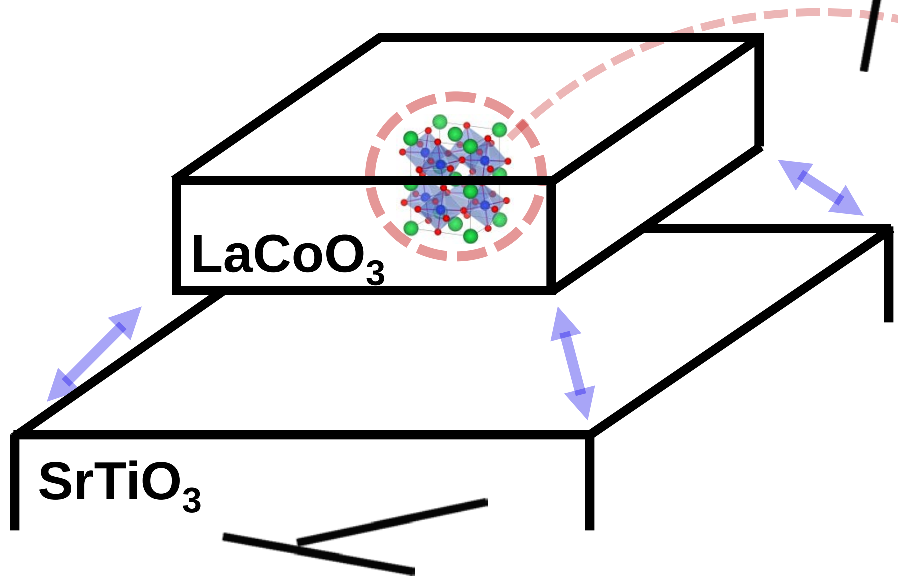

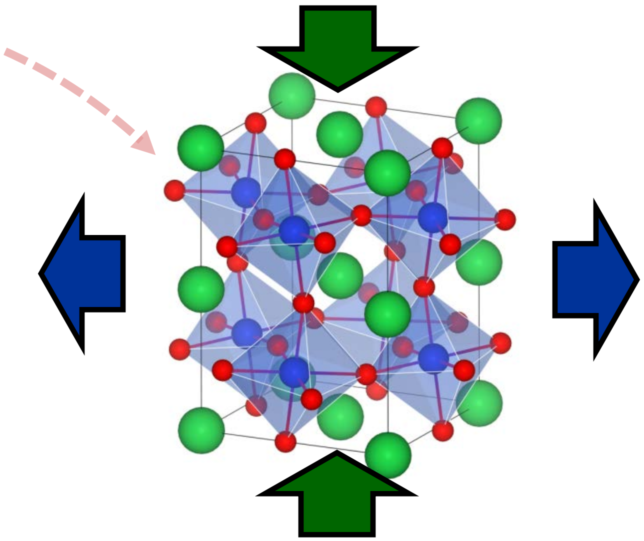

- Corner-sharing octahedral network with relatively rigid CoO_6 units under epitaxial stress

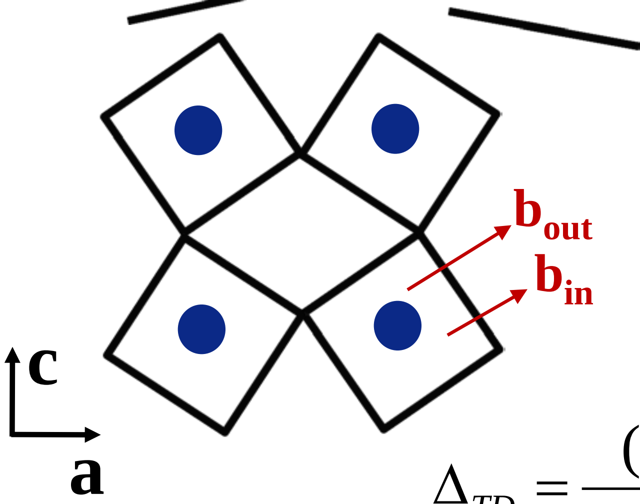

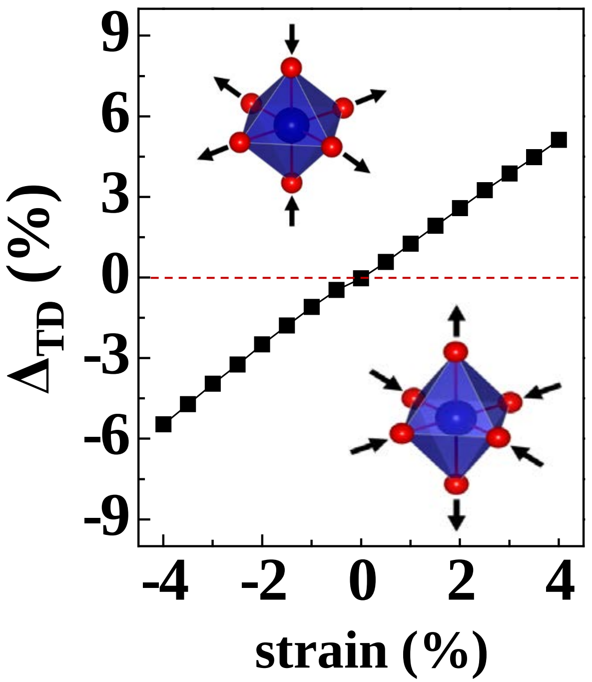

$$\Delta_{TD} = \frac{(b_{in} - b_{out})}{|b_{in} + b_{out}|/2}$$

Bond lengths and angles

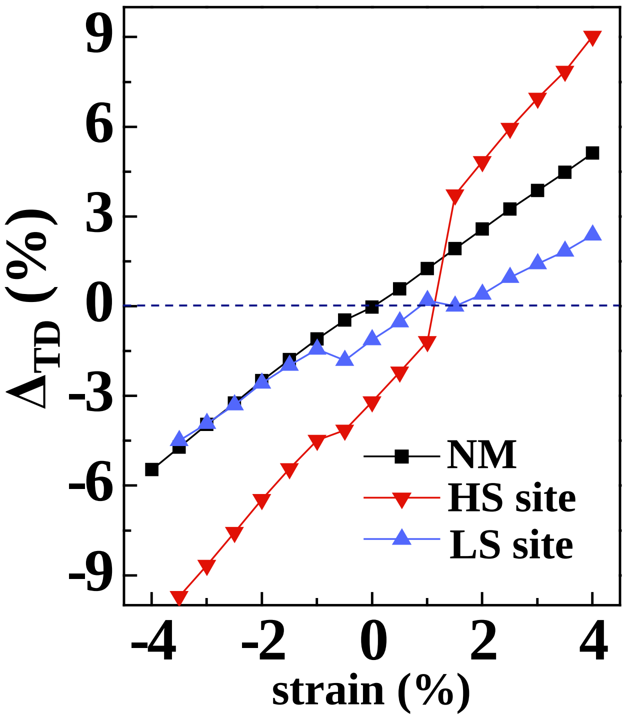

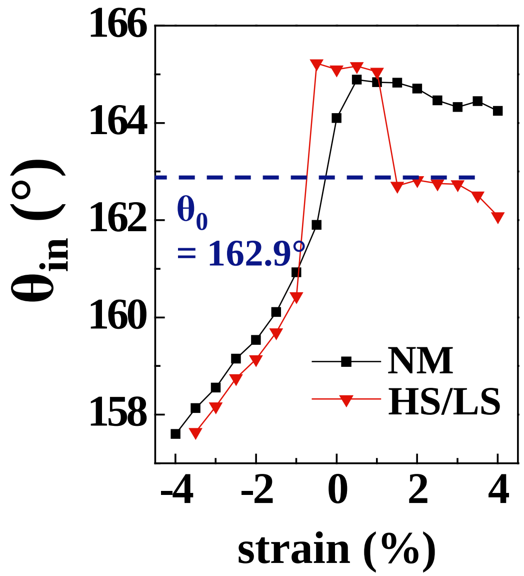

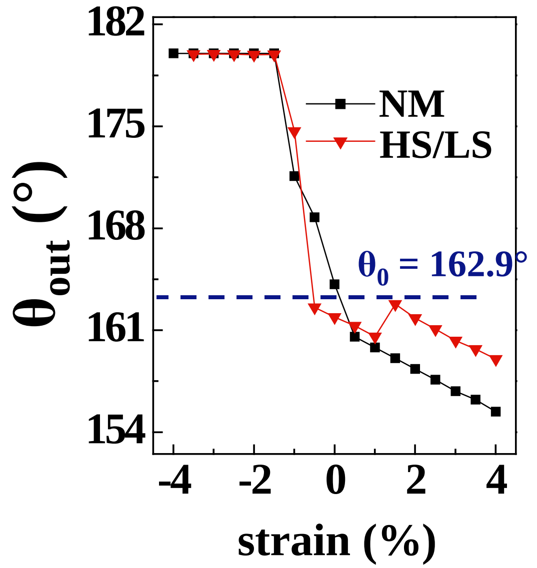

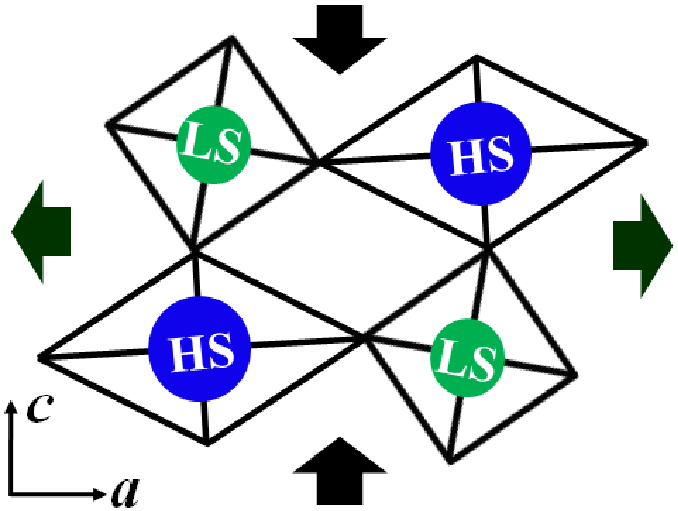

Voltage-switchable magnetoresistance in $LaCoO_3$

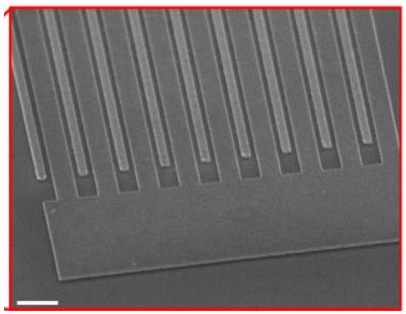

SEM image of device

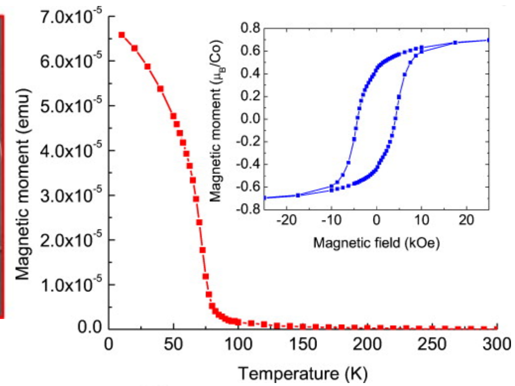

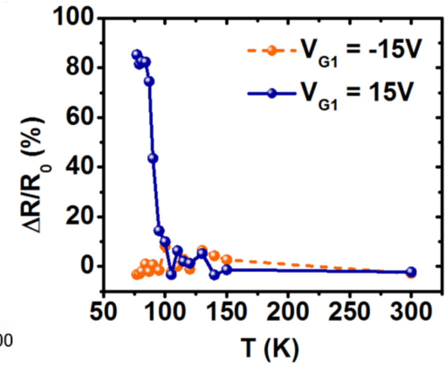

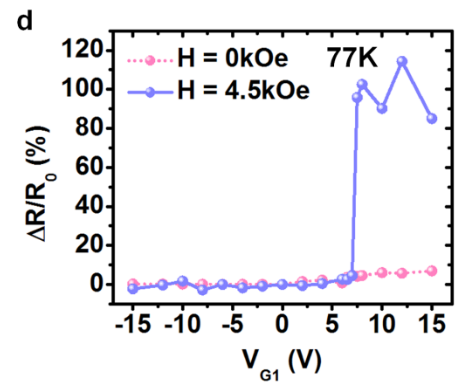

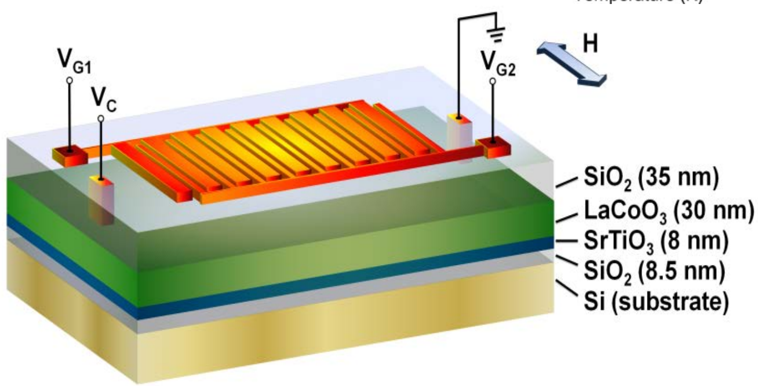

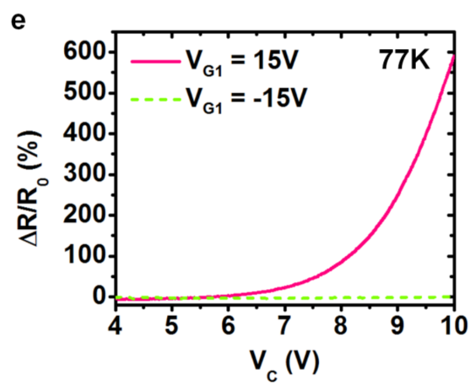

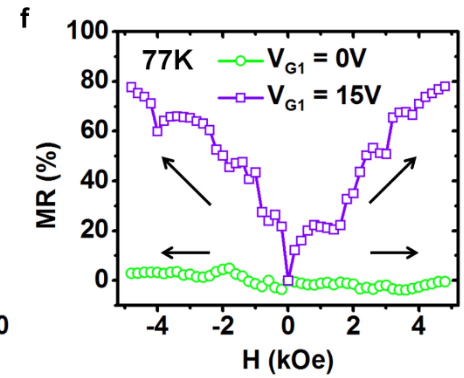

Normally nonmagnetic $LaCoO_3$ becomes ferromagnetic below 85 K under tensile strain

No magnetoresistance above T_C for both voltage polarities
Magnetoresistance observed only below T_C and for only positive voltage
Critical voltage needed to observe magentoresistance

In collaboration with Ed Yu, UT Austin

Summary

- **First demonstration of epitaxial growth of magnetic $LaCoO_3$ on silicon.**

- **High quality crystalline $LaCoO_3$ layer epitaxially strained to underlying $SrTiO_3$ buffer (XRD, TEM, XPS), T_C ~ 85 K (SQUID)**

- **Beyond biaxial tensile strain of 2.5% local magnetic moments, originating from HS (S=2) states of Co^{3+} ions, emerge in the LS Co^{3+} matrix.**
- **The HS/LS state is insulating.**

- **The stabilization of the FM state is attributed to increased compliance of LCO when it has higher concentration of HS Co^{3+} ions. Despite the energy cost to excite LS Co^{3+} to HS state, LCO chooses this option and gains energy above tensile strain of 2.5% owing to the softness of the HS CoO_6 clusters.**

- **In contrast, compressive strain could not produce a magnetic state in LCO.**